

## Supporting Information

### The Principle of Detailed Balancing, the Iron-Catalyzed Disproportionation of Hydrogen Peroxide, and the Fenton Reaction

David M. Stanbury

Dept. of Chemistry and Biochemistry, Auburn University, Auburn, AL 36849, USA

#### Contents

1.	Improper reversible steps	2
2.	Illegal loops not involving peroxo-Fe complexes	5
3.	Illegal loops involving peroxo-Fe complexes	15
4.	Illegal loops involving Fe-ligand complexes.	26
5.	Heterogeneous violations.	29
	References	30

#### Inventory of improper reversible steps and illegal loops

An extensive survey of publications on the mechanism of iron-catalyzed decomposition of  $\text{H}_2\text{O}_2$ , the Fenton reaction, and related processes has revealed a host of different mechanisms having various improper reversible steps and illegal loops. Here we provide descriptions of each of these, summarize the publications where they occur, and analyze their significance. Suitable corrections are provided for many of these violations based on the specifics described in section 2. For convenience here we often denote reversible steps as "loops", even though they do not really consist of multiple steps. In many cases we used numerical methods to simulate the loops or mechanisms in order to assess the quantitative effects of modifications to comply with the principle of detailed balancing. These simulations were performed with COPASI.<sup>1</sup>

Many of the mechanisms proposed in the literature are incomplete in that they lack certain essential acid/base reactions. We have taken the liberty of assuming that the authors implicitly recognized the participation of three specific reactions: the acid dissociation of  $\text{HO}_2^\bullet$  and  $\text{H}_2\text{O}_2$  (steps 1.1 and 1.2 in Table 1) and the acid dissociation of  $\text{H}_2\text{O}$ . Inclusion of these steps is required in order for DETBAL to identify loops properly.

Non-mass-action kinetics is used in many of the publications discussed below. One of the ways this can occur is for a species to be a reactant in the balanced stoichiometry but not to be included in the rate law. This situation is indicated in many of the loops below by including the species within brackets, e.g. [+  $\text{H}^+$ ].

## 1. Improper reversible steps

Loop 1



There are many publications that include this pair of reactions in the proposed mechanism, assigning second-order kinetics to both steps.<sup>2-44</sup> The  $\text{H}^+$  in the second step is bracketed to indicate that it is required for the stoichiometry but does not appear in the rate law. This reaction pair corresponds to a reversible equilibrium, but it violates the principle of detailed balancing because the rate expressions in the forward and reverse directions are second order, which disagrees with the form of the equilibrium expression. As discussed in section 2.2, the first step has an inverse acid dependence. The use of second-order kinetics would be acceptable only if conditional kinetics were used, but the nomenclature implies that conditional kinetics is not being used.

Simulations show the serious effect of this violation. These simulations use the brief mechanism in Zhou et al. 2021 (their eqs 1 - 8),<sup>40</sup> supplemented with the acid dissociation equilibria of  $\text{H}_2\text{O}_2$  and  $\text{HO}_2\cdot$  and with a rapid  $\text{OH}\cdot$  scavenger step. Under initial conditions of 1 mM  $\text{Fe}^{2+}$ , 1 mM  $\text{Fe}^{3+}$ , 10 mM  $\text{H}_2\text{O}_2$ , and 1 M scavenger the half life for consumption of  $\text{H}_2\text{O}_2$  is the same at pH 1 and pH 2. When the rate constant for the reaction of  $\text{Fe}^{3+}$  with  $\text{H}_2\text{O}_2$  is increased by a factor of 10 on going from pH 1 to pH 2 as required by the known inverse acid dependence of this step and the principle of detailed balancing, the half life for  $\text{H}_2\text{O}_2$  consumption decreases by a factor of 10.

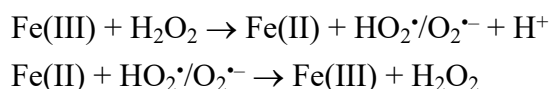
Conditional kinetics is used in several publications that have mechanisms including the above pair of reactions. 1) In one of these Gubler et al. 2011 used conditional kinetics for both steps at pH 0, so the results could be acceptable at pH 0.<sup>25</sup> Unfortunately this paper used the kinetics of Walling and Goosen, so its conditional forward rate constant at pH 0 of  $k = 4 \times 10^{-5} \text{ M}^{-1} \text{ s}^{-1}$  disagrees with the value discussed above (section 2.2). 2) The mechanism of Zhang et al. 2018 includes the above two reactions if the stoichiometry of the second step is corrected as shown. It uses conditional kinetics at pH 2, which could be acceptable. However, the ratio of the forward and reverse rate constants disagrees by a factor of 14 with the conditional equilibrium constant given in section 2.5.<sup>32</sup>

Conditional kinetics is also used in several publications where the above pair of reactions are modified by replacing  $\text{Fe}^{3+}$  and  $\text{Fe}^{2+}$  by  $\text{Fe(III)}$  and  $\text{Fe(II)}$ . In one of these Farias et al. 2009 used conditional kinetics for both steps, even though the second step was shown as having  $\text{H}^+$  as

a reactant.<sup>45</sup> In another, Qiu et al. 2015 used conditional kinetics at pH 3, but the ratio of the two rate constants disagrees with the conditional equilibrium constant by a factor of 17.<sup>46</sup> In a third, Wong and Kjeang 2015 used conditional kinetics with the rate constants of Gubler et al. at pH 0. However, there is no indication that the experiments were performed at pH 0.<sup>47</sup> In a fourth publication Cui et al. 2017 used conditional kinetics but with rate constants at an unspecified pH. The actual pH ranged from 2.75 to 7.5 in the experiments, which is clearly inconsistent with their use of rate constants at a specific pH.<sup>48</sup> In a fifth publication, Pan et al. 2021 used conditional kinetics at pH 6 to model the reaction in the presence of humic acid, which is acceptable in principle.<sup>49</sup> However, they used rate constants from a prior study that was conducted at pH 3 without humic acid, and they assumed that the rate constants were the same at pH 6. Moreover, the reaction mixtures were iron-containing suspensions, but the model did not include any steps involving the colloid particles.

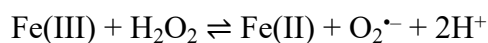
Chang & Chern 2010 assigned mass-action rate constants for both of the above reactions.<sup>50</sup> Although this assignment does not violate the principle of detailed balancing, it does disagree with the known inverse-acid dependence of the first step and the known second-order rate law for the second step.

## Loop 2



The nomenclature of this reversible pair is a mixture of conditional and non-conditional kinetics because of the inclusion of H<sup>+</sup> in the first step. This pair of steps would be in compliance with the principle of detailed balancing if the H<sup>+</sup> produced in the first step is removed, the rate constants are conditional, and the rate constant ratio agrees with the conditional equilibrium constant. The loop has its origin in a publication by Kwan and Voelker, where the second reaction contained a typographical error showing the product as HO<sub>2</sub> rather than H<sub>2</sub>O<sub>2</sub>; this publication provided values for the conditional rate constants at pH 3, 4 and 5.<sup>51</sup> This pair of reactions appears in the mechanisms of several subsequent publications with the rate constants of Kwan and Voelker.<sup>52-59</sup> It also appears in Oueslati et al. 2018 for experiments at pH 6 with rate constants from an unknown source;<sup>60</sup> this raises a serious question about how rates could be specified for Fe(III) at pH 6 given its insolubility. In all cases the ratio of the forward and reverse rate constants disagrees with the conditional equilibrium constant calculated from eq 34.

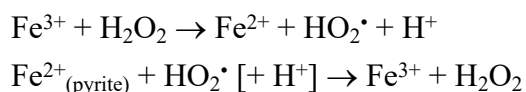
## Loop 3



Stoichiometrically this reversible step is consistent with the principle of detailed balancing, but the conditional kinetics implied by the use of Fe(III) and Fe(II) in this loop is not consistent with the designation of  $\text{O}_2^{\bullet-} + 2\text{H}^+$  as products. The loop appears in Zong et al. 2020, where conditional kinetics was used for both the forward and reverse steps.<sup>61</sup> The model was applied to experiments at pH 8 at which the conditional equilibrium constant is  $2.2 \times 10^{-12}$  as calculated by eq 34. The ratio of the rate constants used by Zong et al. is  $2.5 \times 10^{-10}$ , which is in poor agreement with the conditional thermodynamic value. Of greater concern is that the model was used with no consideration of the high insolubility of Fe(III) at this pH. This step may be irrelevant to the results of the model because the model includes rapid and irreversible binding of Fe(II) and Fe(III) by an excess of the ligand TPP.

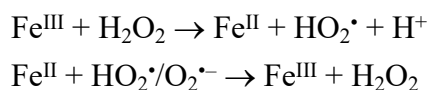
This step also appears in the model of Wang et al. 2021, which was applied at pH 3, 5, and 7.<sup>62</sup> pH-independent second-order rate constants were used in both the forward and reverse directions. This description is thus in contradiction with both conditional and non-conditional kinetics.

#### Loop 4



This pair of steps appears in Farshchi et al. 2019 and is a loop if  $\text{Fe}^{2+}_{(\text{pyrite})}$  is taken to mean aqueous  $\text{Fe}^{2+}$  originating from pyrite.<sup>63</sup> The rate constants assigned are second-order and thus must refer to aqueous species. Since both rate equations are second order they disagree with the form of the equilibrium expression. A further concern is that the mechanism includes the thermal oxidation of water by  $\text{Fe}^{3+}$  as discussed in section 2.6.

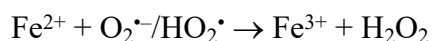
#### Loop 5



This pair of reactions appears in Miller et al. 2018.<sup>64</sup> The first step is ambiguous in that  $\text{Fe}^{\text{III}}$  implies conditional kinetics whereas the specification of  $\text{HO}_2^{\bullet} + \text{H}^+$  as products implies non-

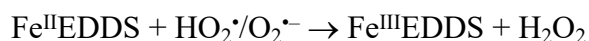
conditional kinetics. No rate eqs are provided. Nevertheless, the stoichiometries of the two steps imply different paths for the two steps, which violates the principle of detailed balancing.

Loop 6



These two reactions appear in the model of He & Zhou 2017 for the electro-Fenton process.<sup>65</sup> Despite the charge designations of the iron species and the designation of  $\text{HO}_2^\bullet$  and  $\text{H}^+$  as products in the first step, the rate equations are conditional at pH 2.5, 3, and 4 and come from Kwan and Voelker 2002.<sup>51</sup> The ratio of these forward and reverse rate constants disagrees quite significantly with the thermodynamic conditional equilibrium constants calculated from eq 34.

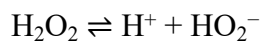
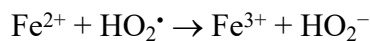
Loop 7



Here EDDS refers to the ligand ethylenediamine-*N,N'*-disuccinic acid. This pair of steps appears in Zhang et al. 2016 and in Checa-Fernandez et al. 2021.<sup>66, 67</sup> The nomenclature is a mixture of conditional and non-conditional terms, and as no rate equations are provided it is unclear whether the authors intended conditional kinetics or not. As written these two steps are inconsistent with the principle of detailed balancing.

## 2. Illegal loops not involving peroxo-Fe complexes

Loop 8



This illegal loop is the one that occurs most widely, originating in the highly influential publication of Barb et al. 1951.<sup>68</sup> It is illegal because  $\text{H}_2\text{O}_2$  is reduced directly to  $\text{HO}_2^\bullet$  but  $\text{HO}_2^\bullet$  is oxidized via  $\text{HO}_2^-$  to  $\text{H}_2\text{O}_2$ . As is shown below, if mass-action kinetics is used, correcting it to conform with the principle of detailed balancing can lead to qualitative changes in simulations of

mechanisms where it occurs. Even though the loop is conceptually incorrect, if non-mass-action kinetics is used it is possible to obtain quantitatively accurate results with this loop. The loop appears as shown in a few publications.<sup>68–70</sup> If the acid dissociation of  $\text{H}_2\text{O}_2$  is included it appears in at least 49 publications.<sup>71–121</sup> There are two publications where it appears if the stoichiometry of the first step in the loop is corrected as shown above and the acid dissociation of  $\text{H}_2\text{O}_2$  is included.<sup>122, 123</sup> If the second step is corrected as shown above and the third step is added it appears in two other publications.<sup>124, 125</sup>

If  $\text{Fe}^{3+}$  is replaced by  $\text{Fe(III)}$  and  $\text{Fe}^{2+}$  by  $\text{Fe(II)}$  the loop appears in ten other publications.<sup>126–135</sup> Although conditional nomenclature is used in these papers, only one of them actually uses conditional kinetics.<sup>127</sup>

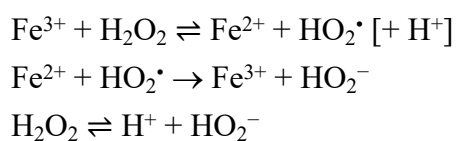
Mechanisms using mass-action kinetics in this loop are incorrect because the first step has an inverse acid dependence as discussed in section 2.2. If we disregard this concern, the consequences of this illegal loop in a mass-action mechanism can be explored by performing simulations of the loop based on the mechanism and parameters of a publication by Lin and Guroi 1998.<sup>78</sup> These simulations used  $K_a(\text{H}_2\text{O}_2) = 2.2 \times 10^{-12}$  M and initial conditions of  $10 \mu\text{M}$   $\text{Fe}^{3+}$ ,  $10 \mu\text{M}$   $\text{Fe}^{2+}$ , pH 2, 10 mM  $\text{H}_2\text{O}_2$ . Simulation of just the illegal loop yields a half-rise time for  $\text{HO}_2^\bullet$  of 0.06 s and  $[\text{HO}_2^\bullet]_{\text{ss}} = 1.7 \times 10^{-11}$  M. With  $K^\circ = 2.2 \times 10^{-12}$  M for step 1 from Table 1, a value of  $9.3 \times 10^8 \text{ M}^{-2} \text{ s}^{-1}$  is obtained for the reverse rate constant of the first step in the loop. Combination with the other rate constant in the loop yields a value of  $9.9 \times 10^5 \text{ M}^{-1} \text{ s}^{-1}$  for the reverse rate constant of the second step. Simulation with these two reverse rate constants included yields a half-rise time for  $\text{HO}_2^\bullet$  of 8 ms and  $[\text{HO}_2]_\infty = 2.1 \times 10^{-12}$  M. Simulation of the unmodified original whole mechanism of the  $\text{Fe}^{3+}$ -initiated decomposition of  $\text{H}_2\text{O}_2$  with the above parameters show a zero-order decay of  $\text{H}_2\text{O}_2$  with a first half-life of 40 s. When the above reverse rate constants in the loop are included the decay of  $\text{H}_2\text{O}_2$  becomes approximately pseudo-first order and the first half life increases to 60 s. These results show that inclusion of the above illegal loop in mass-action mechanisms can be quantitatively significant. At least 34 publications have mechanisms using mass-action kinetics in this loop.<sup>75, 78, 80, 81, 83, 86–89, 91, 93, 94, 96, 98, 100–102, 106, 107, 110, 111, 114, 117, 120, 122, 123, 126–128, 130–133, 136</sup> One of these shows the steps in the loop but then excludes them from the final model.<sup>96</sup>

There are a few publications that use the inverse acid dependence in the first step of the loop (non-mass-action kinetics).<sup>68, 71–74</sup> The principle of detailed balancing with this inverse acid dependence in the forward direction requires an acid-independent rate law for the reverse, which is the same as the second step. Simulations with the rate constants of Barb et al. and under a variety of conditions show that there is no significant change in the final concentration of  $\text{HO}_2^\bullet$  when the loop is corrected by including the reverse rate constants for the first two steps. This unusual result arises because the rate law and rate constant for the reverse of the first step are the

same as for the forward second step and the third step is much faster than the others. The apparent illegality of the loop could have been avoided if the authors had simply made the first step reversible with non-mass-action kinetics in both directions; with this adjustment the second step could have been omitted.

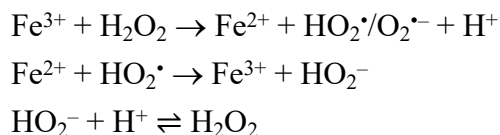
There are two publications that use conditional kinetics in this loop. In principle this method could lead to acceptable quantitative results because the conditional rate constants could reflect the non-mass-action kinetics described above. One of these publications uses the rate constants in a lumped empirical expression, so it is not possible to determine whether the outcome is affected.<sup>80</sup> The other publication uses rate constants for the first two steps of the loop that have a ratio that disagrees with the conditional equilibrium constant by a factor of 17, which is clearly an unacceptable deviation.<sup>127</sup>

#### Loop 9



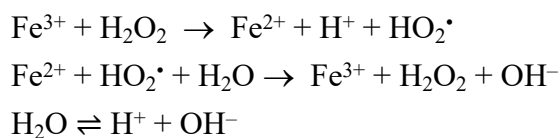
This variation on Loop 8 differs by having the first step reversible. It appears in Chi et al. 2011 if the last step is added.<sup>23</sup> A confusing set of possibly conditional rate constants is provided in Table 1 of that publication. The second step is redundant because it is essentially the same as the reverse of the first step. The fitted rate constants in later tables are conditional and refer to iron complexes.

#### Loop 10



This is another variation of Loop 8, differing by specifying the products of the first step as  $\text{HO}_2^\bullet/\text{O}_2^{\bullet-}$  rather than  $\text{HO}_2^\bullet$ . It appears in Wang et al. 2018 if the acid dissociation of  $\text{H}_2\text{O}_2$  is added;<sup>137</sup> the source of the two rate constants is not indicated, nor is a pH specified. It is unclear whether conditional kinetics is being applied.

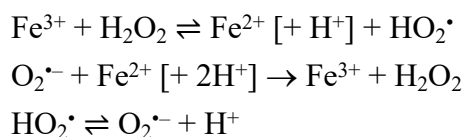
#### Loop 11



This loop violates the principle of detailed balancing because the oxidation of  $\text{H}_2\text{O}_2$  produces  $\text{H}^+$  whereas the reverse consumes  $\text{H}_2\text{O}$ . The loop appears in several publications.<sup>138–141</sup> These four papers use mass-action kinetics despite the known inverse acid dependence of the first step. The rate constants in two of these publications have rate constants in the unusual dimensions of  $\text{m}^3$ , not  $\text{L}$ .<sup>140, 141</sup>

If  $\text{Fe}^{3+}$  and  $\text{Fe}^{2+}$  are replaced by  $\text{Fe(III)}$  and  $\text{Fe(II)}$  respectively, the loop appears in Gholami et al. 2020 if the second reaction is corrected as shown and the acid dissociation of water is added.<sup>142</sup> This paper uses conditional kinetics with the incorrect rate constants of Kwan and Voelker 2002 (see section 2.4).

## Loop 12



This is the first of several illegal loops in which  $\text{O}_2^{\cdot-}$  is oxidized to  $\text{H}_2\text{O}_2$  but  $\text{H}_2\text{O}_2$  is reduced to  $\text{HO}_2\cdot$ . The loop appears in many publications.<sup>3, 4, 6–8, 10, 11, 13, 14, 16, 17, 19, 20, 23, 24, 34, 35, 38, 39, 44</sup> If the acid dissociation of  $\text{HO}_2\cdot$  is added it also appears in two other publications.<sup>15, 31</sup>

Since this loop has  $\text{H}^+$  as a bracketed reactant, none of the papers using this loop use mass-action kinetics. All of the papers cited above provide rate constants for the steps in the loop. Unless conditional kinetics is used, the first step must incorporate the acid dependence properly in the rate equations. Of the above papers, only two of them explicitly use conditional kinetics.<sup>11, 23</sup> All of the other papers cited use second-order kinetics for the forward and reverse of the first step and thus they violate the principle of detailed balancing.

Apart from the problems with the first step in the loop, a partial solution to the illegality of the loop could be the elimination of the second step. Simulations of the loop with the rate constants in Herrmann et al. 2000,<sup>4</sup> 10 mM  $\text{H}_2\text{O}_2$ , 1 mM  $\text{Fe}^{2+}$ , 1 mM  $\text{Fe}^{3+}$ , and pH 1 - 3 show that the steady-state  $\text{HO}_2$  concentration is the same whether step 2 is included or not. At pH 5 the steady-state  $\text{HO}_2$  concentration increases by a factor of 10 when the second step is omitted. These results show that the second step cannot be neglected at high pH. To bring the loop into

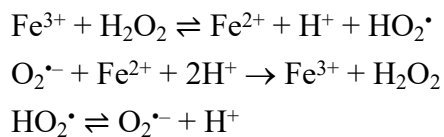


compliance with the principle of detailed balancing the second step would need to be made reversible; this could be achieved relatively easily by rewriting the second step as in eq 22 and including the hydrolysis of  $\text{Fe}^{3+}$ .

The experiments of Rivas et al. 2001 were all performed at pH 3.2 and the pH remained constant during the kinetic runs.<sup>6</sup> It is conceivable that the authors intended to use conditional kinetics; if this is the case then the ratio of their forward and reverse rate constants for the first step in the loop deviates from the conditional equilibrium constant by a factor of 18. This deviation could, in part, explain the failure of their model to fit some of the experimental results.

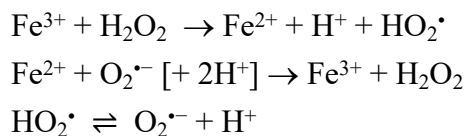
Loop 12 appears in Chi et al. 2011 with conditional kinetics at pH 3.4 for the first step.<sup>23</sup> Two sets of rate constants for the mechanism were developed: in Model A the ratio of the forward and reverse rate constants of the first step in the loop is  $1.7 \times 10^{-8}$  and in Model B it is  $5.0 \times 10^{-8}$ , neither of which is in acceptable agreement with the conditional equilibrium constant calculated from eq 34 as  $4.8 \times 10^{-11}$ .

#### Loop 13



This illegal loop differs from Loop 12 by including  $2\text{H}^+$  as a reactant for the second step, leading to a 4th-order rate law. This loop appears in only one publication, with mass-action kinetics for the whole mechanism.<sup>50</sup> However, some of the rate constants taken from the literature have incorrect dimensions: the reverse rate constant for the first step is assigned third-order dimensions whereas the source<sup>143</sup> provides the same numerical value for a second-order rate law; the rate constant for the second step is given as 4th-order whereas the source<sup>144</sup> provides the same numerical value but as a second-order rate constant.

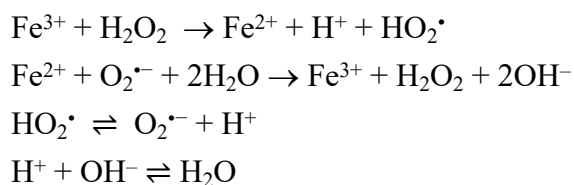
#### Loop 14



This illegal loop differs from Loop 12 by having the first step irreversible. It appears in at least 14 publications.<sup>2, 12, 43, 87, 99, 101, 145–152</sup> Despite its known inverse acid dependence, the first

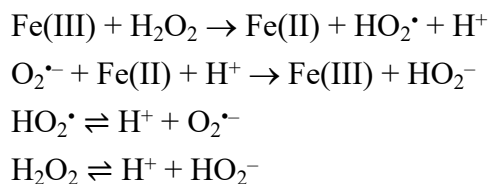
step is assigned mass-action kinetics in all of the above publications except for one,<sup>101</sup> which does not provide rate eqs. Two of these publications are also marred by having mechanisms that include the thermal one-electron oxidation of water by Fe<sup>3+</sup> (see section 2.6).<sup>150, 152</sup> Resolution of the illegality of this loop could be achieved by including the reverse of the first two steps, the rate constants being calculated from the forward rate constants and the equilibrium constants in Table 1.

#### Loop 15



Two publications have mechanisms that include this illegal loop if the last step is added.<sup>140, 141</sup> Both papers use mass-action kinetics for the first step despite its known inverse acid dependence. The second step seems rather unlikely and might be better written as in eq 16. The loop could then be made legal by including the hydrolysis of Fe<sup>3+</sup> and the reverse of the first two steps. Note that the rate constants are provided in units of moles/m<sup>3</sup> rather than the usual moles/l.

#### Loop 16

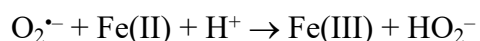
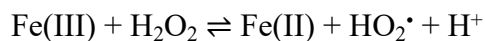


Illegal Loop 16 appears in Yu et al. 2018 if the last step is added.<sup>130</sup> It also appears in two other publications if Fe(III) and Fe(II) are replaced by Fe<sup>3+</sup> and Fe<sup>2+</sup>,<sup>90, 153</sup> neither of these two publications provides rate equations.

Yu et al. 2018 assign second-order rate constants to the 1st and 2nd steps, which is possible only if conditional kinetics is being used.<sup>130</sup> With the conditional equilibrium constant for the first step at pH 3 of  $9.3 \times 10^{-11}$  as calculated from eq 34, the conditional forward rate constant of Yu et al. requires a conditional reverse rate constant of  $2.2 \times 10^7 \text{ M}^{-1} \text{ s}^{-1}$ . Simulations of this loop at pH 3 with 1 mM Fe(III), 1 mM Fe(II) and 10 mM H<sub>2</sub>O<sub>2</sub> with the rate constants of Yu et al. show that the steady-state HO<sub>2</sub> concentration decreases from 4 μM to 0.03 μM when

the reverse of the first step is included. These results show that illegal loops involving conditional kinetics can lead to highly incorrect outcomes.

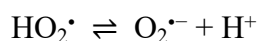
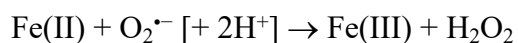
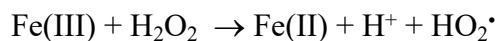
#### Loop 17



Loop 17 differs from Loop 16 by having the first step reversible. It appears in the heavily cited review of Pignatello et al. 2006 if the last two steps are added (pages 3 and 13)<sup>154</sup> and in Cui et al. 2017 if the last step is added.<sup>48</sup> The paper of Cui et al. uses second-order rate constants for the forward and reverse of the first step, which can only be correct if conditional kinetics is used. However, no specific pH is specified; furthermore, the ratio of these two rate constants is  $1.7 \times 10^{-8}$ , which is much larger than the thermodynamic conditional equilibrium constant at any pH.

If Fe(III) and Fe(II) are replaced by Fe<sup>3+</sup> and Fe<sup>2+</sup> and the last two steps are added, this loop appears in three publications.<sup>22, 26, 40</sup> All three papers use the same second-order rate constants for the first two steps. The ratio of the forward and reverse rate constants for the first step is  $8.3 \times 10^{-9}$ , which is at least 50-fold greater than the thermodynamic conditional equilibrium constant at any pH. This disagreement renders moot any efforts to repair the illegal loop by adding the reverse of the second step.

#### Loop 18

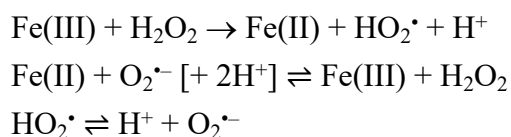


This loop is a puzzling blend of conditional and non-conditional nomenclature. Nevertheless, it violates the principle of detailed balancing by having a path from H<sub>2</sub>O<sub>2</sub> to O<sub>2</sub><sup>•-</sup> via HO<sub>2</sub><sup>•</sup> whereas the path from O<sub>2</sub><sup>•-</sup> to H<sub>2</sub>O<sub>2</sub> bypasses HO<sub>2</sub><sup>•</sup>. It appears in five publications.<sup>131, 155-158</sup> Ouyang et al. 2020 provides no kinetics.<sup>158</sup> Zimbron & Reardon 2009 use conditional kinetics for the first step but differentiate between HO<sub>2</sub><sup>•</sup> and O<sub>2</sub><sup>•-</sup> for the second step;<sup>156</sup> this raises difficulties in formulating a suitable rate expression for the reverse of the second step. The

same difficulties are raised by the mechanism of Yang et al. 2019.<sup>131</sup> Although Fang et al. 2020 use oxidation-state nomenclature, the sources of their rate constants are consistent with Fe<sup>3+</sup> and Fe<sup>2+</sup> as reactants;<sup>157</sup> their experiments were performed over the pH range 2.5 - 4, but they used an acid-independent rate law for the first step in the loop. Because of these complications there is no simple way to correct this illegal loop in these publications.

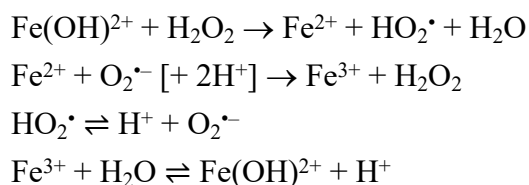
With Fe(II) replaced by Fe<sup>2+</sup> and omission of H<sup>+</sup> in the first two steps the loop appears in Möller & Mauersberger 1992; it is not clear what rate constants were used.<sup>159</sup>

#### Loop 19



This illegal loop appears in Wang et al. 2021.<sup>62</sup> Although conditional kinetics was used in portions of the mechanism it was not used for the steps in this loop. This disagrees with the known inverse acid dependence of the first step, and as noted for Loop 3 this also makes the second step incorrect.

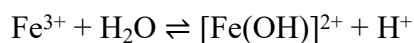
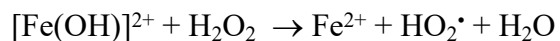
#### Loop 20



This loop is the first of several that explicitly involve hydrolyzed forms of Fe(III). It appears in Hermann et al. 1999 and Herrmann et al., 2000.<sup>3,4</sup> It also appears in Deguillaume et al. 2004 if the acid dissociation of HO<sub>2</sub><sup>•</sup> is added.<sup>13</sup> The first step has a calculated equilibrium constant of 3.1 × 10<sup>-10</sup>, and the forward rate constant used by Herrmann et al. is 2 × 10<sup>-3</sup> M<sup>-1</sup> s<sup>-1</sup>. These quantities require a reverse rate constant of 6.5 × 10<sup>6</sup> M<sup>-1</sup> s<sup>-1</sup>. Simulations of the loop were performed with the rate constants of Herrmann et al. at pH 3 with 1 mM Fe<sup>2+</sup>, 1 mM Fe<sup>3+</sup>, 10 mM H<sub>2</sub>O<sub>2</sub>, and they showed that HO<sub>2</sub><sup>•</sup> is produced with a half life of 7.2 ms and a steady-state concentration of 1.3 × 10<sup>-10</sup> M. When the requisite first step rate constant was added the HO<sub>2</sub><sup>•</sup> half life decreased to 0.13 ms and the steady-state concentration decreased to 1.9 × 10<sup>-12</sup> M. These results are sufficient to show that including the reverse of the first step has large

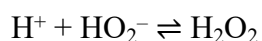
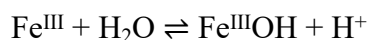
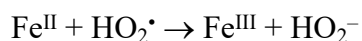
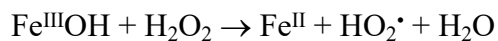
consequences, but a full correction of the loop would also require adding the reverse of the second step.

#### Loop 21



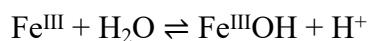
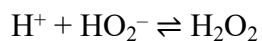
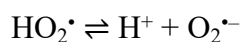
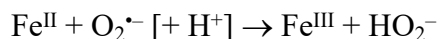
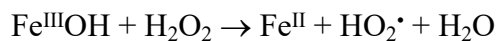
This loop appears in three publications on atmospheric chemistry.<sup>3, 4, 13</sup> In addition to being an illegal loop because of the irreversibility of the first step, the second step violates the principle of detailed balancing by having non-conditional forward and reverse rate expressions that disagree with the equilibrium expression.

#### Loop 22



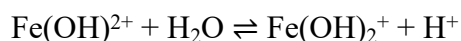
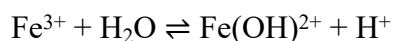
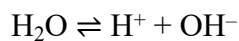
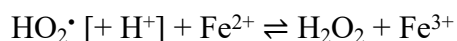
Loop 22 appears in Vorontsov 2019 and uses mass-action kinetics.<sup>160</sup> The significance of the  $\text{Fe}^{\text{III}}\text{OH}$  nomenclature in the first step is unclear. The "mechanism" provided in Scheme 1 of Vorontsov 2019 includes oxidation of  $\text{H}_2\text{O}_2$  by direct oxidation as in the first step in this loop and also via a peroxo-iron complex as in Loop 41; inclusion of these parallel paths and a large array of rate constants for the various steps is an indication that the "mechanism" is actually an uncritical compilation of various reported steps.

#### Loop 23



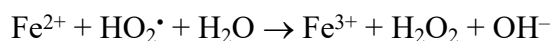
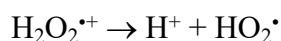
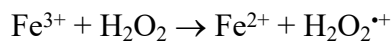
Loop 23 appears in Vorontsov 2019.<sup>160</sup> The comments regarding Loop 22 apply here as well and indicate that Loop 23 should not be taken seriously.

Loop 24



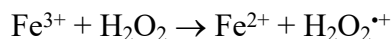
This loop appears in three publications.<sup>3, 4, 13</sup> In addition to being illegal because of the irreversibility of the first step, the second step in all three papers uses second-order non-conditional kinetics for the forward and reverse directions and thus is incompatible with its equilibrium expression.

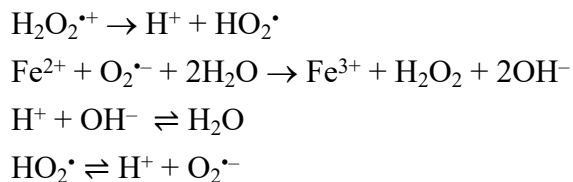
Loop 25



This loop appears in Graedel et al. 1986.<sup>161</sup> The steps in the loop obey mass-action kinetics although the first step should have an inverse acid dependence. It is clear that  $\text{H}_2\text{O}_2^{*+}$  is a strong acid, and hence its  $\text{p}K_a$  has not been measured. This requires  $E^\circ(\text{H}_2\text{O}_2^{*+}/\text{H}_2\text{O}_2) > 1.46 \text{ V}$  and thus  $K_{\text{eq}} < 2.2 \times 10^{-12}$  for the first step. These authors use a rate constant of  $600 \text{ M}^{-1} \text{ s}^{-1}$  for the first step, which requires a reverse rate constant greater than  $2.7 \times 10^{14} \text{ M}^{-1} \text{ s}^{-1}$ . There is clearly an error in the mechanism as this greatly exceeds the diffusion limit. The production of  $\text{H}_2\text{O}_2^{*+}$  in the first step is a concept that has not achieved wide acceptance and probably should be disregarded or modified. The review of Sychev and Isak 1995 reports a  $K_a$  value for  $\text{H}_2\text{O}_2^{*+}$ , but this must be an error because this species is not mentioned in the cited sources.<sup>162</sup>

Loop 26



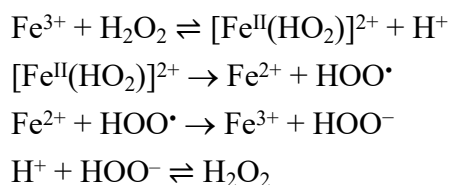


This loop appears in Graedel et al. 1986.<sup>161</sup> As noted for Loop 25, the participation of  $\text{H}_2\text{O}_2^{\bullet+}$  suggests that the first step in this loop should be disregarded or modified.

### 3. Illegal loops involving peroxo-Fe complexes

As noted above, the kinetics of oxidation of  $\text{H}_2\text{O}_2$  by Fe(III) has an inverse acid dependence, which means that mass-action kinetics is unable to simulate the rates properly for mechanisms that include eq 1. This difficulty is removed by including the formation of  $[\text{Fe}^{\text{III}}(\text{HO}_2)]^{2+}$  along the  $\text{H}_2\text{O}_2$  oxidation pathway as is characteristic of many of the loops in this section. Although this is an improvement, the many illegal loops in this section show that adherence to the principle of detailed balancing is still important.

#### Loop 27



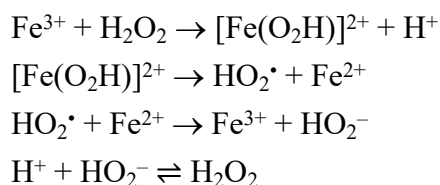
This loop is illegal because it converts  $\text{H}_2\text{O}_2$  to  $\text{HOO}^{\bullet}$  via a peroxo-Fe complex but the reverse bypasses the complex. It is the most commonly encountered illegal loop involving a peroxo-Fe complex, appearing in four publications as shown<sup>162–165</sup> and in another 22 publications if the acid dissociation of  $\text{H}_2\text{O}_2$  is added.<sup>79, 166–186</sup> The loop also appears in De Laat & Le 2005 if their species  $\text{I}_a$  is understood to be  $[\text{Fe}^{\text{II}}(\text{HO}_2)]^{2+}$  and if Fe(II) in the third step is replaced by  $\text{Fe}^{2+}$ .<sup>187</sup> It appears in Shen et al. 2021 if Fe(II) in the third step is replaced by  $\text{Fe}^{2+}$ .<sup>188</sup> It appears in Arts et al. 2021 if the first two eqs are corrected as shown, the acid dissociation of  $\text{H}_2\text{O}_2$  is included, and  $\text{Fe}^{3+}$  and  $\text{Fe}^{2+}$  are replaced by Fe(III) and Fe(II);<sup>134</sup> although this loop appears in the tabular description of the mechanism, it was not used in their simulation models. Siedlecka and Stepnowski 2006 mistakenly assign the forward rate constant for the first step to the equilibrium constant for that reaction.<sup>178</sup>

The principle of detailed balancing enables the reverse rate constant of the third step to be calculated from its forward rate constant and its equilibrium constant given in Table 1. This equilibrium constant, in combination with the other rate and equilibrium constants in the loop

enables the reverse rate constant for the second step to be calculated. Simulations of the mechanisms of Kozlov et al. 1974 and of Kiwi et al. 2000 show that the half-life for decomposition of H<sub>2</sub>O<sub>2</sub> is not significantly affected by including the reverse rate constants for the second and third steps.<sup>163, 165</sup> This outcome is similar to that seen for Loop 8 and has an analogous explanation: the rate constant for the third step is almost identical to the calculated reverse rate constant for the second step. A legal and more economical presentation of the mechanism would have been to omit the third step in the loop and to assign its rate constant to the reverse of the second step.

A very different outcome is revealed by simulations of the photochemical mechanism of Herrera et al. 1999 for the oxidation of reactive dyes.<sup>164</sup> Here, the simulated rate of oxidation of the dyes is unaffected by inclusion of the reverse rate constants for the second and third steps, but the rate is also unaffected by the presence of H<sub>2</sub>O<sub>2</sub>! In this mechanism the steps involving H<sub>2</sub>O<sub>2</sub> can be omitted because the rate of consumption of the dyes is simply the rate of the photochemical reduction of Fe<sup>3+</sup> by the dyes.

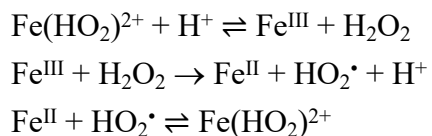
#### Loop 28



This illegal loop is the same as Loop 27 except that the first step is irreversible. It provides an example of the substantial quantitative changes that can occur when the illegalities in a loop involving a peroxo-Fe complex are corrected. The complete loop appears in Lunar et al. 2000.<sup>189</sup> If the acid dissociation of H<sub>2</sub>O<sub>2</sub> is added it also appears in 9 other publications.<sup>105, 107, 190–196</sup> Of the two publications that provide rate constants for the first three steps, one mistakenly transcribed the equilibrium constant for the first step as a rate constant.<sup>107</sup> The other illustrates the serious consequences of violating the principle of detailed balancing.<sup>192</sup> Simulations of the loop with the parameters of this latter publication at pH 2.8, 1 mM Fe<sup>3+</sup> and 7.5 mM H<sub>2</sub>O<sub>2</sub> generate a steady-state H<sub>2</sub>O<sub>2</sub> concentration of 1.3 μM. When the reverse rate constant for the third step is included as required by the thermodynamic equilibrium constant in Table 1 and the reverse rate constants for the first and second step are included as required by the loop, the final HO<sub>2</sub> concentration decreases by a factor of 13 to 98 nM.

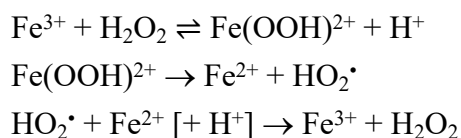
#### Loop 29





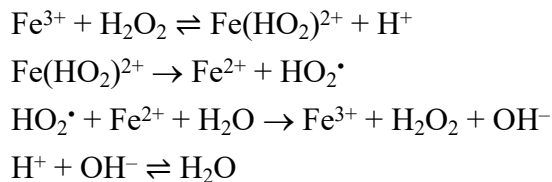
This illegal loop appears in Andreozzi et al. 2000.<sup>197</sup> Although these authors use oxidation-state nomenclature, it is clear from the rate constants used that Fe<sup>III</sup> and Fe<sup>II</sup> in their mechanism are actually Fe<sup>3+</sup> and Fe<sup>2+</sup> and that conditional kinetics is not being used. The constants provided in Andreozzi et al. require a value of  $2.4 \times 10^8 \text{ M}^{-2} \text{ s}^{-1}$  for the reverse of the second step. In simulating just the three steps in the loop, the effect of including this reverse rate constant depends on the rate constants selected for the first step; the ratio of these rate constants must yield the specified equilibrium constant. Under the initial conditions of 1 M H<sup>+</sup>, 1 μM Fe(III), 1 mM H<sub>2</sub>O<sub>2</sub> the concentration of HO<sub>2</sub><sup>•</sup> reaches a steady state at about 200 s. The steady-state concentration is  $1.7 \times 10^{-10} \text{ M}$  with a rate constant of  $365 \text{ M}^{-1} \text{ s}^{-1}$  for the reverse of the first step and with the reverse of the second step set to zero; the equilibrium concentration decreases to  $9 \times 10^{-11} \text{ M}$  when the required reverse of the second step is included. This choice of the rate constant for the reverse of the first step is based on typical rates of substitution at Fe<sup>3+</sup>. The small effect of including the reverse of the second step arises because the other steps are reversible and considerably faster. The same small effect is seen when the second step is excluded entirely, showing that the loop arises because of the inclusion of this unnecessary step.

### Loop 30



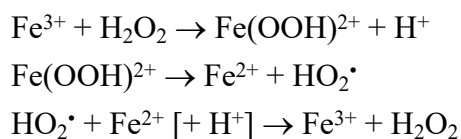
This illegal loop appears in Wiegand et al. 2017 if Fe<sup>III</sup> and Fe<sup>II</sup> in the original last eq are replaced by Fe<sup>3+</sup> and Fe<sup>2+</sup>.<sup>198</sup> This paper uses non-mass-action kinetics, the third step in the loop being independent of [H<sup>+</sup>]. A simple correction to make the loop legal would be to make the second step reversible, assign its reverse rate constant the value of the rate constant for the third step, and delete the third step. This correction should not introduce any significant numerical differences and it would make the mechanism simpler.

### Loop 31



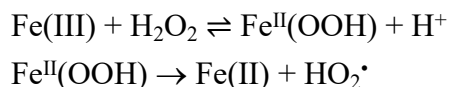
This loop appears in Table 3 of Gasmi et al. 2020 and Table 1 of Kerboua et al. 2021 if the acid dissociation of water is added.<sup>140, 199</sup> The mechanism in these two papers uses mass-action kinetics. The forward rate constant provided by Gasmi et al. for the third step is  $1.2 \times 10^3 \text{ mol}^{-1} \text{ m}^3 \text{ s}^{-1}$  ( $1.2 \times 10^6 \text{ mol}^{-1} \text{ l s}^{-1}$ ), which requires a reverse rate constant of  $2.7 \times 10^8 \text{ mol}^{-2} \text{ l}^2 \text{ s}^{-1}$  when combined with the equilibrium constant in Table 1. The other parameters in the loop then require a reverse rate constant for the second step of  $3.5 \times 10^6 \text{ mol}^{-1} \text{ l s}^{-1}$ . Simulations of the loop with initial conditions of pH 3, 0.35 mM  $\text{H}_2\text{O}_2$ , 2  $\mu\text{M}$   $\text{Fe}^{3+}$  and 2  $\mu\text{M}$   $\text{Fe}^{2+}$  and excluding the reverse of steps 2 and 3 yields a 0.36 s rise time for attaining a steady-state  $\text{HO}_2$  concentration of  $2 \times 10^{-12} \text{ mol}$ . Including the reverse steps reduces the rise time to 0.1 s and the final concentration decreases by a factor of 3. This small effect arises because the third step is essentially the same as the reverse of the second step and the rate constants are quite similar. As with Loop 30, Loop 31 could be made legal without introducing any significant numerical changes by making the second step reversible and removing the third step.

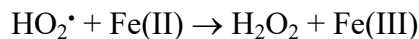
### Loop 32



This loop appears in Qin et al. New J. Chem. 2020 and uses non-mass-action kinetics.<sup>200</sup> These authors mistakenly regarded the first step to be irreversible and assigned it a rate constant that is numerically equal to the equilibrium constant. The loop also appears in Ghiselli et al. 2004 but with no kinetics.<sup>201</sup> Even if the first step is corrected to be reversible the loop is still illegal because the other two steps are irreversible. A complete solution would be to have the first two steps reversible and delete the third step.

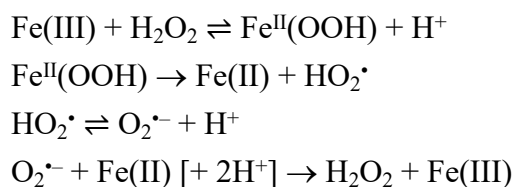
### Loop 33





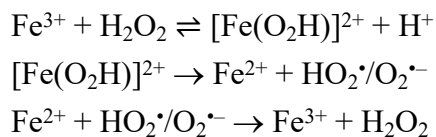
This loop appears in Kang & Hua 2005 and is a perplexing mixture of conditional and non-conditional nomenclature.<sup>202</sup> The third step appears to be unbalanced with respect to protons, but the use of oxidation-state nomenclature (Fe(III)) allows for Fe to be a proton donor. Rate constants are provided, but even if conditional kinetics is used there is still the violation that oxidation of H<sub>2</sub>O<sub>2</sub> proceeds via an iron complex but the reverse does not. It is difficult to assess the quantitative implications of this illegal loop because of the wide range of rate constants specified by the authors for the second step.

#### Loop 34



This illegal loop also appears in Kang & Hua 2005, has the same steps for reduction of Fe(III), but differs in the path of oxidation of Fe(II).<sup>202</sup> As with Loop 33, it violates the principle of detailed balancing by having an irreversible path from Fe(III) and H<sub>2</sub>O<sub>2</sub> to Fe(II) and HO<sub>2</sub><sup>•</sup> via a peroxo-iron complex but a reverse path that does not.

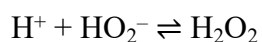
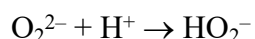
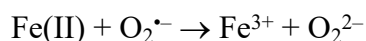
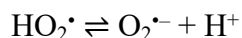
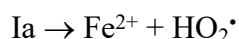
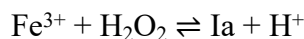
#### Loop 35



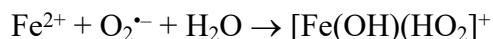
This is not exactly a stoichiometric loop because H<sup>+</sup> occurs only in the first step. It is virtually a loop because the use of HO<sub>2</sub><sup>•</sup>/O<sub>2</sub><sup>•-</sup> nomenclature obscures the participation of H<sup>+</sup>. Nevertheless, it is illegal because the route from H<sub>2</sub>O<sub>2</sub> to HO<sub>2</sub><sup>•</sup>/O<sub>2</sub><sup>•-</sup> passes through [Fe(O<sub>2</sub>H)]<sup>2+</sup> but the reverse does not. This loop appears in Chen et al. 2021 (Table S2).<sup>203</sup> It could yield acceptable numerical results, since the third step is essentially the same as the reverse of the second step, but this would require the pH dependence of the second and third steps to be compatible. These authors specify a pH-dependent rate constant for the third step, corresponding to reaction via HO<sub>2</sub><sup>•</sup> or O<sub>2</sub><sup>•-</sup>. However, the two rate constants differ by only a factor of 10 while

the  $pK_a$  of  $\text{HO}_2^\bullet$  is  $-4.8$ . This difference requires the rate constant for the second step to be pH-dependent also, but it was specified to be pH-independent.

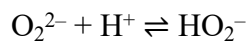
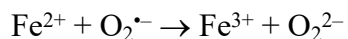
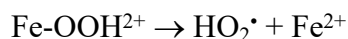
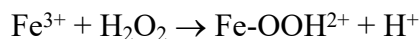
### Loop 36



Loop 36 is a loop if Fe(II) in the fourth reaction is understood to be  $\text{Fe}^{2+}$ . This loop appears in De Laat & Le 2005<sup>187</sup> and De Laat & Le, 2006.<sup>204</sup> It appears in Shen et al. 2021 if  $\text{I}_a$  is understood to be  $\text{Fe}(\text{HO}_2)^{2+}$  and Fe(II) in the last step is written as  $\text{Fe}^2$ .<sup>188</sup> It also appears in Rojas et al. 2010 if the last two eqs are added,  $\text{I}_a$  is written as  $\text{Fe}(\text{HO}_2)^{2+}$ , and Fe(II) is written as  $\text{Fe}^{2+}$ .<sup>185</sup> As is discussed above (section 2.4), the fourth step (formation of  $\text{O}_2^{2-}$ ) can be ruled out in view of its high estimated endothermicity. This difficulty could be eliminated by replacing the fourth step with formation of a peroxo-Fe complex as discussed in section 2.2:

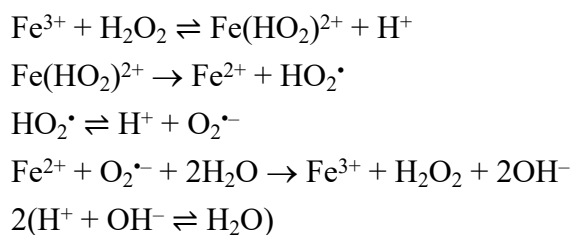


### Loop 37



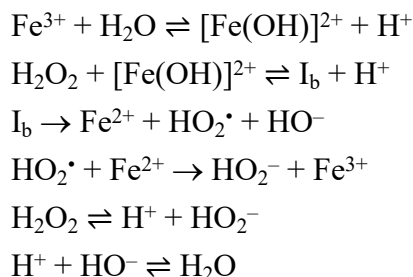
Loop 37 appears in Benitez et al. 2007 if the last three steps are added.<sup>205</sup> It differs from Loop 36 by having the first step irreversible, which is clearly an error. Moreover, the third step can be ruled out as noted for Loop 36.

### Loop 38



This illegal loop can be repaired by including the reverse of the second and fourth steps. The reverse of the second step is described in section 2.3. The reverse rate constant of the fourth step can be calculated from the other rate and equilibrium constants. As noted in section 2.4, the fourth step in this illegal loop is not an elementary step. This illegal loop appears in Gasmi et al. 2020 and in Kerboua et al. 2021 if the acid dissociation of water is included.<sup>140, 199</sup>

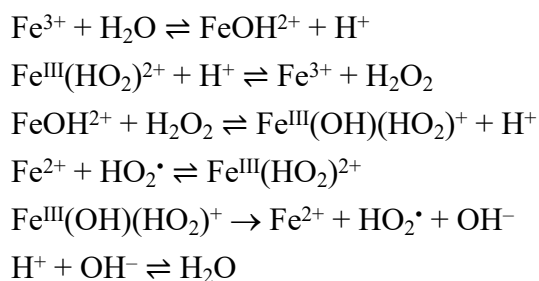
#### Loop 39



The loop appears in De Laat & Le 2005 and in De Laat and Le 2006 if Fe(II) is replaced by Fe<sup>2+</sup> in the 4th step.<sup>187, 204</sup> It also appears in Rojas et al. 2010 if the species I<sub>b</sub> is understood to be Fe(OH)(HO<sub>2</sub>)<sup>+</sup> and the last two steps are added.<sup>185</sup> It appears in Shen et al. 2021 if I<sub>b</sub> is understood to be Fe(OH)(HO<sub>2</sub>)<sup>+</sup> and Fe(II) is replaced by Fe<sup>2+</sup> in the 4th step.<sup>188</sup>

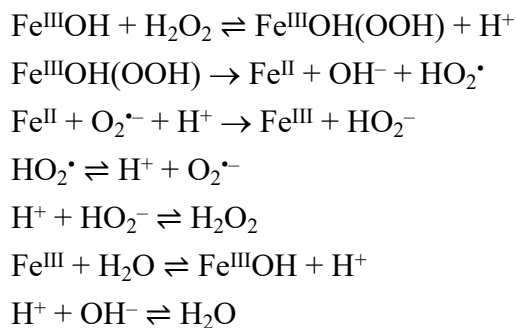
Simulation of this loop with the parameters of De Laat and Le 2006, 1 mM Fe<sup>3+</sup>, 50 mM H<sub>2</sub>O<sub>2</sub> and pH 2 yields a steady-state HO<sub>2</sub><sup>•</sup> concentration of 19 nM. The reverse of the 4th step has a rate constant of 1.2 × 10<sup>6</sup> M<sup>-1</sup> s<sup>-1</sup> as required by its equilibrium constant in Table 1; with this equilibrium constant and the other parameters in the loop a value of 8.5 × 10<sup>16</sup> M<sup>-2</sup> s<sup>-1</sup> is calculated for the reverse rate constant of the third step. With these two additional rate constants the loop becomes legal and the simulated final HO<sub>2</sub><sup>•</sup> concentration increases from 19 to 71 nM. An alternative solution could be to remove the fourth step and replace the third step by eq 13 and its reverse.

#### Loop 40



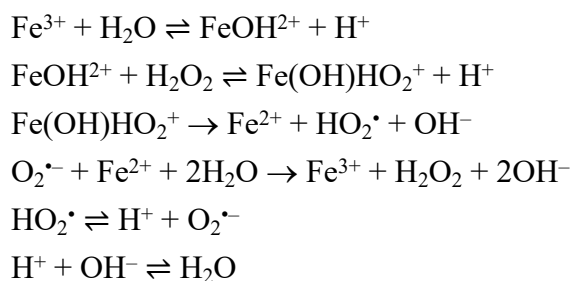
This illegal loop appears in De Laat & Gallard 1999, Gallard and De Laat 2000, and in Giannakis et al. 2016 if the acid dissociation of water is included.<sup>206–208</sup> It appears in Giannakis et al. 2017 if the first and last steps are added.<sup>209</sup> The simplest repair of this loop would be to make the penultimate step reversible with a reverse rate constant as discussed in section 2.2.

#### Loop 41



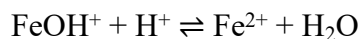
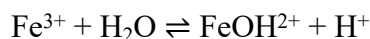
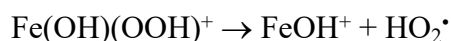
Loop 41 appears in Vorontsov 2019 if the acid dissociation of water is added.<sup>160</sup> As noted for Loops 22 and 23, Loop 41 should not be taken seriously.

#### Loop 42



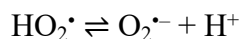
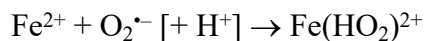
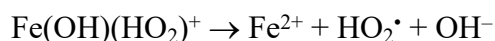
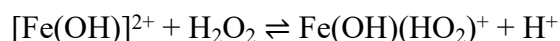
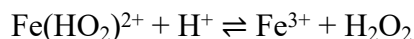
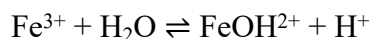
This illegal loop appears in Gasmi et al. 2020 if the last step is added; the mechanism uses mass-action kinetics.<sup>140</sup> The rate constants are in units of  $\text{m}^3$  rather than the usual  $\text{l}$ . As noted in Table 1 the equilibrium constant for the fourth step is  $2.9 \times 10^{-12} \text{M}^2$ , and this requires its reverse rate constant to be  $3.4 \times 10^{18} \text{M}^{-3} \text{s}^{-1}$  when combined with the forward rate constant. A value of  $6.1 \times 10^{16} \text{M}^{-2} \text{s}^{-1}$  can then be derived for the reverse rate constant for the third step. Simulations of the loop are significantly affected by inclusion of these two reverse rate constants: with  $1 \text{mM Fe}^{2+}$ ,  $1 \text{mM Fe}^{3+}$ ,  $0.35 \text{mM H}_2\text{O}_2$  at pH 3 the final  $\text{HO}_2^\bullet$  concentration decreases from  $6.5 \times 10^{-13} \text{M}$  to  $1.7 \times 10^{-13} \text{M}$  upon inclusion of the reverse rate constants.

#### Loop 43



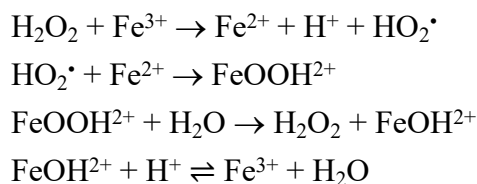
Loop 43 appears in Wiegand et al. 2017 if  $\text{Fe}^{\text{II}}$  and  $\text{Fe}^{\text{III}}$  in the original third step are replaced by  $\text{Fe}^{2+}$  and  $\text{Fe}^{3+}$  and the last two steps are added.<sup>198</sup> The parameters provided by Wiegand et al. in combination with the equilibrium constants in Table 1 require a reverse rate constant of  $6 \times 10^{11} \text{M}^{-1} \text{s}^{-1}$  for the second step, which greatly exceeds the plausible substitution rate at  $[\text{Fe}(\text{OH})]^+$ .

#### Loop 44



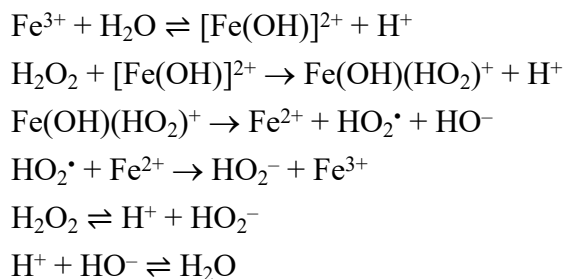
This loop appears in Giannakis et al. 2016 (their Table 3) if the acid dissociation of water is added.<sup>208</sup> A proper resolution of this loop should await redetermination of the rate constant for the fourth step as discussed in section 2.2.

#### Loop 45



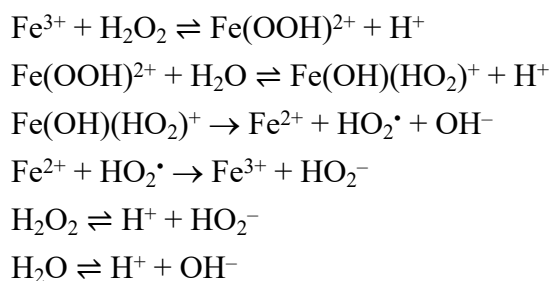
Loop 45 appears in Martin et al. 1989 if the last step is added.<sup>210</sup> It violates the principle of detailed balancing by oxidizing  $\text{H}_2\text{O}_2$  directly to  $\text{HO}_2\cdot$  but reducing  $\text{HO}_2\cdot$  via a peroxo-iron complex. Moreover, this paper assigns a second-order rate law to the first step despite the known inverse acid dependence.

#### Loop 46



This illegal loop appears in Velo-Gala et al. 2014 if the first and last two steps are added.<sup>107</sup> It also appears in Siedlicka & Stepnowski, Water Environ. Res., 2007 if the stoichiometry of the second step is corrected and the first step and last two steps are added.<sup>192</sup> Both of these papers mistakenly assigned a rate constant rather than an equilibrium constant to the second step.

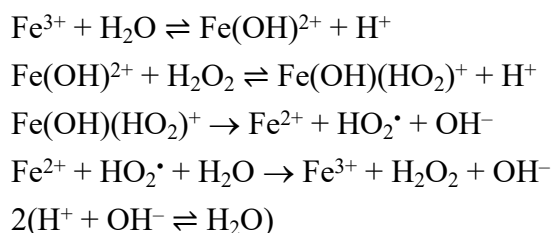
#### Loop 47





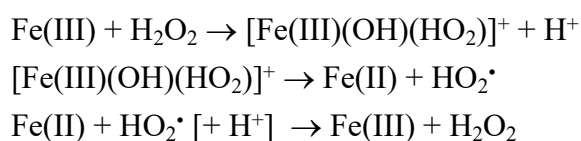
Loop 47 occurs in Siedlecka & Stepnowski 2006 and in Siedlecka et al. J. Haz. Mater. 2007 if the first and second reactions are corrected as shown and the last two reactions are added.<sup>178 179</sup> In view of the confusion regarding the first two reactions it is not clear whether the loop actually represents the authors' intentions.

Loop 48



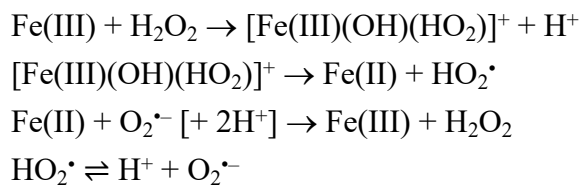
This illegal loop appears in Gasmi et al. 2020 and in Kerboua et al. 2021 if the acid dissociation of water is included.<sup>140, 199</sup> The reverse rate constant for the third step can be calculated as described in section 2.2, and the reverse of the fourth step is defined by the other rate constants and equilibrium constants in the loop.

Loop 49



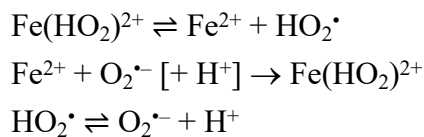
With three irreversible steps it is difficult to suggest a simple repair for this illegal loop. Amme et al. 2005 used this loop in a kinetic model of UO<sub>2</sub> dissolution;<sup>211</sup> because of the use of this and illegal Loop 50 the derived rate constants must be deemed questionable.

Loop 50



As with Loop 49, this illegal loop is part of a mechanism proposed by Amme et al. 2005 to describe the dissolution of  $\text{UO}_2$ .<sup>211</sup>

Loop 51

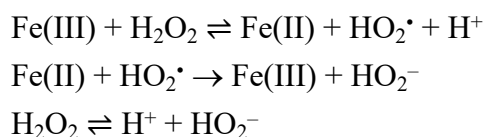


This loop is not strictly within the scope of this Perspective because it does not include the oxidation of  $\text{H}_2\text{O}_2$  by Fe(III). Nevertheless it is illegal, and it appears in several publications.<sup>197, 206–208, 212, 213</sup> It also appears in two other publications if the acid dissociation of  $\text{HO}_2$  is included.<sup>209, 214</sup>

Simulation of the loop with the parameters of De Laat & Gallard 1999 and using  $[\text{Fe}^{2+}]_0$  and  $[\text{Fe}(\text{HO}_2)^{2+}]_0 = 1 \times 10^{-7}$  M showed no change in the final concentration of  $\text{O}_2^{\cdot-}$  if the second step was omitted. Likewise, in simulation of the whole mechanism of De Laat & Gallard (supplemented with the acid dissociation of  $\text{H}_2\text{O}$ ), omission of the second step in this loop had no effect on the half-life of  $\text{H}_2\text{O}_2$  at pH 2 and the conditions of their Figure 1. Evidently, the second step is unnecessary and should be omitted.

**4. Illegal loops involving Fe-ligand complexes.** There has been considerable interest in developing Fenton-type systems that can be used at neutral pH. A significant difficulty at neutral pH is the insolubility of Fe(III). This can be overcome by use of ligands that bind Fe(III) strongly, but these ligands generally require development of new mechanisms. Some examples of illegal loops arising in these new mechanisms are described here. In these examples the mechanisms are conditional in the sense that they refer to specific ligand concentrations.

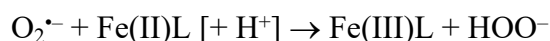
Loop 52



This illegal loop appears in Farinelli et al. 2021 if the last step is added.<sup>215</sup> In Farinelli et al. the species Fe(III) and Fe(II) refer to chitosan complexes. A complication is that the reverse rate constant for the first step is stated to be second order. If pH-conditional kinetics is implied, the loop could be acceptable if the rate constant for the second step were the same as for the

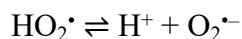
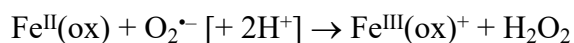
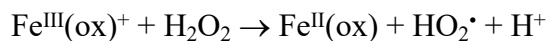
reverse of the first step. However, they differ by about five orders of magnitude, so there is no possible interpretation that makes the loop acceptable.

#### Loop 53



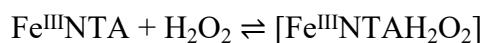
Here, L is the citrate ligand. This loop occurs in Attiogbe & Francis 2011 if the acid dissociation of  $\text{H}_2\text{O}_2$  is included.<sup>216</sup> It has formation of  $\text{O}_2^-$  in the first step because the chemistry is performed in relatively nonacidic media, which is allowed by binding to L. This paper assigns second-order rate laws to the first two steps, but it does not assign rate constants in this loop. One might suppose that the second step could be written as the reverse of the first step, but this would lead to a ratio of rate constants that is dimensionally incompatible with the equilibrium constant.

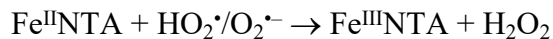
#### Loop 54



This illegal loop is the same as Loop 14 except that it involves oxalato-Fe complexes rather than aquo-Fe complexes. It appears in Fang et al. 2020 with second-order kinetics for the first two steps (Table S1).<sup>157</sup> According to Park et al. 1997,  $E^\circ(\text{Fe}(\text{ox})^{+/0}) = 0.43 \text{ V}$ .<sup>217</sup> This leads to  $K^\circ = 4 \times 10^{-18} \text{ M}$  for the first step. Fang et al. state  $k_f = 2 \times 10^{-3} \text{ M}^{-1} \text{ s}^{-1}$  for the first step, so the reverse rate constant must be  $5 \times 10^{14} \text{ M}^{-2} \text{ s}^{-1}$ . This considerably exceeds the upper limit for a diffusion-controlled termolecular rate constant ( $10^7 \text{ M}^{-2} \text{ s}^{-1}$ ),<sup>218</sup> which implies that the first step must not be an elementary step. Because of the non-mass-action kinetics of the second step, its reverse would have an inverse-square dependence on  $[\text{H}^+]$ . Inclusion of these two reverse steps would make the loop legal.

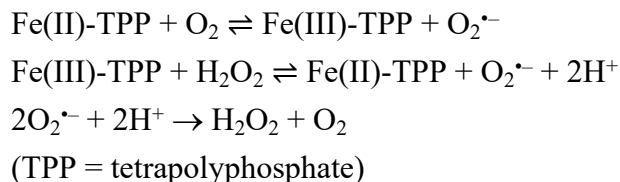
#### Loop 55





This illegal loop appears in De Laat et al. 2011.<sup>219</sup> A simple modification to resolve the illegality would be to rewrite the last step as the reverse of the second step.

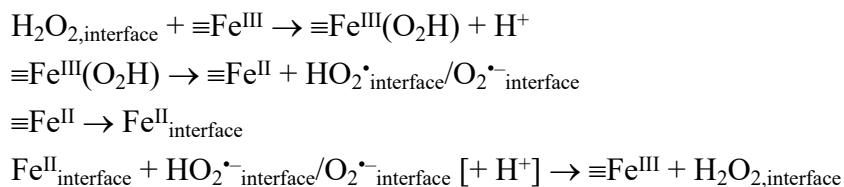
Loop 56



Although this loop is not strictly within the purview of this Perspective, it is included because it involves the oxidation of  $\text{H}_2\text{O}_2$  and the reduction of  $\text{O}_2^{\bullet-}$ . This loop appears in Zong et al. 2020 if the last reaction is corrected as shown above.<sup>61</sup> The rate equations are conditional at pH 8. They require a rate constant of  $9.5 \times 10^{-8} \text{ M}^{-1} \text{ s}^{-1}$  for the reverse of the last step ( $\text{H}_2\text{O}_2 + \text{O}_2$ ). It is difficult to understand how such a low rate constant could be significant, which suggests that some other step is unnecessary. The conditional equilibrium constant for the third step at pH 8 is  $3 \times 10^{16}$  as derived from conventional thermochemical data, but the rate constants provided by Zong et al. for the first two steps yield a conditional equilibrium constant of  $4 \times 10^{14}$ .

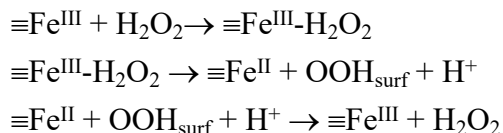
**5. Heterogeneous violations.** Because of the low solubility of Fe(III) in nonacidic media there has been considerable interest in the catalytic properties of precipitated Fe(III) (sludge). In some cases mechanisms have been proposed that include kinetics at the Fe(II) or Fe(III) surface, and in some cases these heterogeneous steps are components of illegal loops. A few examples are included here to illustrate that the principle of detailed balancing is not limited to homogeneous systems. One such example is consists of the following four steps:

Loop 57



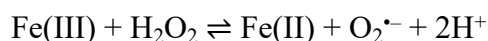
This loop appears in Chen et al. 2021 if the last step is balanced by including  $[+ H^+]$  as shown.<sup>203</sup> Although rate constants are not provided for all of the steps in this loop, the only possible set of rate constants that would make the loop compatible with the principle of detailed balancing would be where one of the rate constants is zero.

#### Loop 58



This illegal loop appears in Wang and Tang 2021.<sup>38</sup> It is presented in general terms for a variety of surfaces and without rate constants. Nevertheless, a scheme which includes these three irreversible steps is prohibited by the principle of detailed balancing.

#### Loop 59



Stoichiometrically this reversible step is consistent with the principle of detailed balancing, but the conditional kinetics implied by the use of Fe(III) and Fe(II) in this loop is not consistent with the designation of  $\text{O}_2^{\bullet-} + 2\text{H}^+$  as products.

This loop appears in Zhang & Yuan 2017,<sup>220</sup> where Fe(II) refers to Fe(II) adsorbed on pyrite and Fe(III) is implied to be in solution. These authors use second-order conditional kinetics for the forward reaction at pH 7 despite the insolubility of Fe(III) at this pH. They also use a conditional rate constant for the reverse step expressed in terms of the concentration of Fe(II) despite it's being adsorbed on the pyrite. In principle the ratio of the rate constants would yield an equilibrium constant that is related to the conditional homogeneous equilibrium constant and the Fe(II) adsorption equilibrium constant; however, the above concerns prevent this analysis.

Wang et al. 2021 also used this step for Fe on pyrite, and they used it in simulations at pH 3,5, and 7.<sup>62</sup> They used pH-independent second-order rate constants in both the forward and reverse directions, which disagrees with the form of the equilibrium expression.

## References

- (1) Hoops, S.; Sahle, S.; Gauges, R.; Lee, C.; Pahle, J.; Simus, N.; Singhal, M.; Xu, L.; Mendes, P.; Kummer, U. COPASI – a COMplex PATHway SIMulator. *Bioinformatics*, **2006**, *22*, 3067-3074. <http://copasi.org>.
- (2) Chen, R.; Pignatello, J. J. Role of Quinone Intermediates as Electron Shuttles in Fenton and Photoassisted Fenton Oxidations of Aromatic Compounds. *Environ. Sci. Technol.*, **1997**, *31*, 2399-2406.
- (3) Herrmann, H.; Ervens, B.; Nowacki, P.; Wolke, R.; Zellner, R. A Chemical Aqueous Phase Radical Mechanism for Tropospheric Chemistry. *Chemosphere*, **1999**, *38*, 1223-1232.
- (4) Herrmann, H.; Ervens, B.; Jacobi, H.-W.; Wolke, R.; Nowacki, P.; Zellner, R. CAPRAM2.3: A Chemical Aqueous Phase Radical Mechanism for Tropospheric Chemistry. *J. Atmos. Chem.*, **2000**, *36*, 231-284.
- (5) Grymonpre, D. R.; Sharma, A. K.; Finney, W. C.; Locke, B. R. The role of Fenton's reaction in aqueous phase pulsed streamer corona reactors. *Chem. Eng. J.*, **2001**, *82*, 189-207.
- (6) Rivas, F. J.; Beltran, F. J.; Frades, J.; Buxeda, P. Oxidation of p-Hydroxybenzoic Acid by Fenton's Reagent. *Water Res.*, **2001**, *35*, 387-396.
- (7) Rivas, F. J.; Beltran, F. J.; Garcia-araya, J. F.; Navarrete, V.; Gimeno, O. Co-oxidation of p-hydroxybenzoic acid and atrazine by the Fenton's like system Fe(III)/H<sub>2</sub>O<sub>2</sub>. *J. Haz. Mater.*, **2002**, *B91*, 143-157.
- (8) Kang, N.; Lee, D. S.; Yoon, J. Kinetic modeling of Fenton oxidation of phenol and monochlorophenols. *Chemosphere*, **2002**, *47*, 915-924.
- (9) Rossetti, G. H.; Albizzati, E. D.; Alfano, O. M. Decomposition of Formic Acid in a Water Solution Employing the Photo-Fenton Reaction. *Ind. Eng. Chem. Res.*, **2002**, *41*, 1436-1444.
- (10) Cheng, S.-A.; Fung, W.-K.; Chan, K.-Y.; Shen, P. K. Optimizing electron spin resonance detection of hydroxyl radical in water. *Chemosphere*, **2003**, *52*, 1797-1805.
- (11) Rivas, F. J.; Beltran, F. J.; Gimeno, O.; Alvarez, P. Treatment of brines by combined Fenton's reagent-aerobic biodegradation II. Process modelling. *J. Haz. Mater.*, **2003**, *B96*, 259-276.
- (12) Druschel, G. K.; Hamers, R. J.; Luther, G. W.; Banfield, J. F. Kinetics and Mechanism of Trithionate and Tetrathionate Oxidation at Low pH by Hydroxyl Radicals. *Aquatic Geochem.*, **2003**, *9*, 145-164.
- (13) Deguillaume, L.; Leriche, M.; Monod, A.; Chaumerliac, N. The role of transition metal ions on HOx radicals in clouds: a numerical evaluation of its impact on multiphase chemistry. *Atmos. Chem. Phys.*, **2004**, *4*, 95-110.
- (14) Rivas, F. J.; Navarrete, V.; Beltran, F. J.; Garcia-Araya, J. F. Simazine Fenton's oxidation in a continuous reactor. *Appl. Catal. B: Environ.*, **2004**, *48*, 249-258.
- (15) Du, Y.; Zhou, M.; Lei, L. Role of the intermediates in the degradation of phenolic compounds by Fenton-like process. *J. Haz. Mater.*, **2006**, *B136*, 859-865.
- (16) Du, Y.; Zhou, M.; Lei, L. Kinetic model of 4-CP degradation by Fenton/O<sub>2</sub> system. *Water Res.*, **2007**, *41*, 1121-1123.
- (17) Chang, M.-W.; Chen, T.-S.; Chern, J.-M. Initial Degradation Rate of p-Nitrophenol in Aqueous Solution by Fenton Reaction. *Ind. Eng. Chem. Res.*, **2008**, *47*, 8533-8541.
- (18) Hermosilla, D.; Cortijo, M.; Huang, C. P. Optimizing the treatment of landfill leachate by

- conventional Fenton and Photo-Fenton processes. *Sci. Total Environ.*, **2009**, *407*, 3473-3481.
- (19) Huang, Y.-H.; Huang, Y.-J.; Tsai, H.-C.; Chen, H.-T. Degradation of phenol using low concentration of ferric ions by the photo-Fenton process. *J. Taiwan Inst. Chem. Eng.*, **2010**, *41*, 699-704.
  - (20) Pontes, R. F. F.; Moraes, J. E. F.; Machulek, A.; Pinto, J. M. A mechanistic kinetic model for phenol degradation by the Fenton process. *J. Haz. Mater.*, **2010**, *176*, 402-413.
  - (21) Umar, M.; Aziz, H. A.; Yusoff, M. S. Trends in the use of Fenton, electro-Fenton and photo-Fenton for the treatment of landfill leachate. *Waste Manag.*, **2010**, *30*, 2113-2121.
  - (22) Jho, E. H.; Singhal, N.; Turner, S. Fenton degradation of tetrachloroethylene and hexachloroethane in Fe(II) catalyzed systems. *J. Haz. Mater.*, **2010**, *184*, 234-240.
  - (23) Chi, G. T.; Nagy, Z. K.; Huddersman, K. D. Kinetic modelling of the Fenton-like oxidation of maleic acid using a heterogeneous modified polyacrylonitrile (PAN) catalyst. *Prog. React. Kinet. Mech.*, **2011**, *36*, 189-214.
  - (24) Fan, C.; Tsui, L.; Liao, M.-C. Parathion degradation and its intermediate formation by Fenton process in neutral environment. *Chemosphere*, **2011**, *82*, 229-236.
  - (25) Gubler, L.; Dockheer, S. M.; Koppenol, W. H. Radical (HO•, H• and HOO•) Formation and Ionomer Degradation in Polymer Electrolyte Fuel Cells. *J. Electrochem. Soc.*, **2011**, *158*, B755-B769.
  - (26) Jho, E.; Singhal, N.; Turner, S. Tetrachloroethylene and hexachloroethane degradation in Fe(III) and Fe(III)-citrate catalyzed Fenton systems. *J. Chem. Technol. Biotechnol.*, **2012**, *87*, 1179-1186.
  - (27) Fan, X.; Hao, H.; Wang, Y.; Chen, F.; Zhang, J. Fenton-Like degradation of nalidixic acid with Fe<sup>3+</sup>/H<sub>2</sub>O<sub>2</sub>. *Environ. Sci. Pollut. Res.*, **2013**, *20*, 3649-3656.
  - (28) Shi, J.; Ai, Z.; Zhang, L. Fe@Fe<sub>2</sub>O<sub>3</sub> core-shell nanowires enhanced fenton oxidation by accelerating the Fe(III)/Fe(II) cycles. *Water Res.*, **2014**, *59*, 145-153.
  - (29) Wang, Z.; Liu, J. New insight into photochemical oxidation of Fe(II): The roles of Fe(III) and reactive oxygen species. *Catal. Today*, **2014**, *224*, 244-250.
  - (30) Chandesris, M.; Medeau, V.; Guillet, N.; Chelghoum, S.; Thoby, D.; Fouda-Onana, F. Membrane degradation in PEM water electrolyzer: Numerical modeling and experimental evidence of the influence of temperature and current density. *Int. J. Hydrogen Energy*, **2015**, *40*, 1353-1366.
  - (31) Zhou, W.; Gao, J.; Zhao, H.; Meng, X.; Wu, S. The role of quinone cycle in Fe<sup>2+</sup>-H<sub>2</sub>O<sub>2</sub> system in the regeneration of Fe<sup>2+</sup>. *Environ. Technol.*, **2017**, *38*, 1887-1896.
  - (32) Zhang, P.; Huang, W.; Ji, Z.; C., Z.; Yuan, S. Mechanisms of hydroxyl radicals production from pyrite oxidation by hydrogen peroxide: Surface versus aqueous reactions. *Geochim. Cosmochim. Acta*, **2018**, *238*, 394-410.
  - (33) Frensch, S. H.; Serre, G.; Fouda-Onana, F.; Jensen, H. C.; Christensen, M. L.; Araya, S. S.; Kaer, S. K. Impact of iron and hydrogen peroxide on membrane degradation for polymer electrolyte membrane water electrolysis: Computational and experimental investigation on fluoride emission. *J. Power Sources*, **2019**, *420*, 54-62.
  - (34) Camacho, F. G.; de Souza, P. A. L.; Martins, M. L.; Beninca, C.; Zanoelo, E. F. A comprehensive kinetic model for the process of electrochemical peroxidation and its application for the degradation of trifluralin. *J. Electroanal. Chem.*, **2020**, *865*, 114163.
  - (35) de Souza, P. A. L.; Camacho, F. G.; da Silva, I. R. A.; Goncalves, F. F.; Beninca, C.; Zanoelo, E. F. An experimental and modeling study of the chain initiation reaction in

- heterogeneous Fenton systems with zero valent iron. *Chem. Eng. J.*, **2020**, 393, 124665.
- (36) Frühwirt, P.; Kregar, A.; Törring, J. T.; Katrasnik, T.; Gescheidt, G. Holistic approach to chemical degradation of Nafion membranes in fuel cells: modelling and predictions. *Phys. Chem. Chem. Phys.*, **2020**, 22, 5647-5666.
- (37) Kregar, A.; Frühwirt, P.; Ritzberger, D.; Jakubek, S.; Katrasnik, T.; Gescheidt, G. Sensitivity Based Order Reduction of a Chemical Membrane Degradation Model for Low-Temperature Proton Exchange Membrane Fuel Cells. *Energies*, **2020**, 13, 5611.
- (38) Wang, J.; Tang, J. Fe-based Fenton-like catalysts for water treatment: Catalytic mechanisms and applications. *J. Molec. Liq.*, **2021**, 332, 115755.
- (39) Li, Y.; Cheng, H. Chemical kinetic modeling of organic pollutant degradation in Fenton and solar photo-Fenton processes. *J. Taiwan Inst. Chem. Eng.*, **2021**, 123, 175-184.
- (40) Zhou, H.; Zhang, H.; He, Y.; Huang, B.; Zhou, C.; Yao, G.; Lai, B. Critical review of reductant-enhanced peroxide activation processes: Trade-off between accelerated Fe<sup>3+</sup>/Fe<sup>2+</sup> cycle and quenching reactions. *Appl. Catal. B: Environ.*, **2021**, 286, 119900.
- (41) Lojo-Lopez, M.; Andrades, J. A.; Egea-Corbacho, A.; Coello, M. D.; Quiroga, J. M. Degradation of simazine by photolysis of hydrogen peroxide Fenton and photo-Fenton under darkness, sunlight and UV light. *J. Water Proc. Eng.*, **2021**, 42, 102115.
- (42) Wu, M. Y.; Cai, Q. Q.; Xu, H. P.; Ong, S. L.; Hu, J. Y. Simulation of FBR-Fenton/GAC process for recalcitrant industrial wastewater treatment with a computational fluid dynamics-kinetic model framework. *Water Res.*, **2021**, 23, 117504.
- (43) Lelieveld, S.; Wilson, J.; Dovrou, E.; Mishra, A.; Lakey, P. S. J.; Shiraiwa, M.; Pöschl, U.; Berkemeier, T. Hydroxyl Radical Production by Air Pollutants in Epithelial Lining Fluid governed by Interconversion and Scavenging of Reactive Oxygen Species. *Environ. Sci. Technol.*, **2021**, 55, 14069-14079.
- (44) Mahtab, M. S.; Islam, D. T.; Farooqi, I. H. Optimization of the process variables for landfill leachate treatment using Fenton based advanced oxidation technique. *Eng. Sci. Technol. Int. J.*, **2021**, 24, 428-435.
- (45) Farias, J.; Albizzati, E. D.; Alfano, O. M. Kinetic study of the photo-Fenton degradation of formic acid. Combined effects of temperature and iron concentration. *Catal. Today*, **2009**, 144, 117-123.
- (46) Qiu, S.; He, D.; Ma, J.; Liu, T.; Waite, T. D. Kinetic Modeling of the Electro-Fenton Process: Quantification of Reactive Oxygen Species Generation. *Electrochim. Acta*, **2015**, 176, 51-58.
- (47) Wong, K. H.; Kjeang, E. Mitigation of Chemical Membrane Degradation in Fuel Cells: Understanding the Effect of Cell Voltage and Iron Ion Redox Cycle. *ChemSusChem*, **2015**, 8, 1072-1082.
- (48) Cui, H.; Gu, X.; Lu, S.; Fu, X.; Zhang, X.; Fu, G. Y.; Qiu, Z.; Sui, Q. Degradation of ethylbenzene in aqueous solution by sodium percarbonate activated with EDDS-Fe(III) complex. *Chem. Eng. J.*, **2017**, 309, 80-88.
- (49) Pan, C.; Jiao, Y.; Kersting, A. B.; Zavarin, M. Plutonium Redox Transformation in the Presence of Iron, Organic Matter, and Hydroxyl Radicals: Kinetics and Mechanistic Insights. *Environ. Sci. Technol.*, **2021**, 55, 1800-1810.
- (50) Chang, M.-W.; Chern, J.-M. Decolorization of peach red azo dye, HF6 by Fenton reaction: Initial rate analysis. *J. Taiwan Inst. Chem. Eng.*, **2010**, 41, 221-228.
- (51) Kwan, W. P.; Voelker, B. M. Decomposition of Hydrogen Peroxide and Organic Compounds in the Presence of Dissolved Iron and Ferrihydrite. *Environ. Sci. Technol.*,



- 2002, 36, 1467-1476. doi.org/10.1021/es011109p.
- (52) Zhang, H.; Lemley, A. T. Reaction Mechanism and Kinetic Modeling of DEET Degradation by Flow-Through Anodic Fenton Treatment (FAFT). *Environ. Sci. Technol.*, **2006**, 40, 4488-4494.
- (53) Duesterberg, C. K.; Waite, T. D. Kinetic Modeling of the Oxidation of p-Hydroxybenzoic Acid by Fenton's Reagent: Implications of the Role of Quinones in the Redox Cycling of Iron. *Environ. Sci. Technol.*, **2007**, 41, 4103-4110.
- (54) Duesterberg, C. K.; Cooper, W. J.; Waite, T. D. Fenton-Mediated Oxidation in the Presence and Absence of Oxygen. *Environ. Sci. Technol.*, **2005**, 39, 5052-5058.
- (55) Duesterberg, C. K.; Waite, D. Process Optimization of Fenton Oxidation Using Kinetic Modeling. *Environ. Sci. Technol.*, **2006**, 40, 4189-4195.
- (56) Zhang, H.; Lemley, A. T. Evaluation of the Performance of Flow-through Anodic Fenton Treatment in Amide Compound Degradation. *J. Agric. Food Chem.*, **2007**, 55, 4073-4079.
- (57) Duesterberg, C. K.; Mylon, S. E.; Waite, T. D. pH Effects on Iron-Catalyzed Oxidation using Fenton's Reagent. *Environ. Sci. Technol.*, **2008**, 42, 8522-8527.
- (58) Georgi, A.; Polo, M. V.; Crincoli, K.; Mackenzie, K.; Kopinke, F.-D. Accelerated Catalytic Fenton Reaction with Traces of Iron: An Fe-Pd-Multicatalysis Approach. *Environ. Sci. Technol.*, **2016**, 50, 5882-5891.
- (59) Zhao, J.; Yang, J.; Ma, J. Mn(II)-enhanced oxidation of benzoic acid by Fe(III)/H<sub>2</sub>O<sub>2</sub> system. *Chem. Eng. J.*, **2014**, 239, 171-177.
- (60) Oueslati, K.; Promeyrat, A.; Gatellier, P.; Daudin, J.-D.; Kondjoyan, A. Stoichio-Kinetic Modeling of Fenton Chemistry in a Meat-Mimetic Aqueous-Phase Medium. *J. Agric. Food Chem.*, **2018**, 66, 5892-5900.
- (61) Zong, Y.; Mao, Y.; Xu, L.; Wu, D. Non-selective degradation of organic pollutants via dioxygen activation induced by Fe(II)-tetrapolyphosphate complexes: Identification of reactive oxidant and kinetic modeling. *Chem. Eng. J.*, **2020**, 398, 125603.
- (62) Wang, W.; He, M.; Ouyang, W.; Lin, C.; Liu, X. Influence of atmospheric surface oxidation on the formation of H<sub>2</sub>O<sub>2</sub> and •OH at the pyrite-water interface: Mechanism and kinetic model. *Chem. Geol.*, **2021**, 571, 120176.
- (63) Farshchi, M. E.; Aghdasinia, H.; Khataee, A. Heterogeneous Fenton reaction for elimination of Acid Yellow 36 in both fluidized-bed and stirred-tank reactors: Computational fluid dynamics versus experiments. *Water Res.*, **2019**, 151, 203-214. doi.org/10.1016/j.watres.2018.12.011.
- (64) Miller, C. J.; Wadley, S.; Waite, T. D. "Fenton, photo-Fenton and Fenton-like processes" in *Advanced Oxidation Processes for Water Treatment*; Stefan, M. I., Ed.; IWA Publishing, London, **2018**; 297-332.
- (65) He, H.; Zhou, Z. Electro-Fenton process for water and wastewater treatment. *Crit. Rev. Environ. Sci. Technol.*, **2017**, 47, 2100-2131.
- (66) Zhang, Y.; Klamerth, N.; Messele, S. A.; Chelme-Ayala, P.; El-Din, M. G. Kinetics study on the degradation of a model naphthenic acid by ethylenediamine-*N,N'*-disuccinic acid-modified Fenton process. *J. Haz. Mater.*, **2016**, 318, 371-378.
- (67) Checa-Fernandez, A.; Santos, A.; Romero, A.; Dominguez, C. M. Application of Chelating Agents to Enhance Fenton Process in Soil Remediation: A Review. *Catalysts*, **2021**, 11, 722.
- (68) Barb, W. G.; Baxendale, J. H.; George, P.; Hargrave, K. R. Reactions of Ferrous and Ferric Ions with Hydrogen Peroxide. Part II. The Ferric Ion Reaction. *Trans. Faraday Soc.*, **1951**,

- 47, 591-616. doi.org/10.1039/TF9514700591.
- (69) Metelitsa, D. I. Mechanisms of the Hydroxylation of Aromatic Compounds. *Russ. Chem. Rev.*, **1971**, *40*, 563-580.
- (70) Lipczynska-Kochany, E. Degradation of Aqueous Nitrophenols and Nitrobenzene by Means of the Fenton Reaction. *Chemosphere*, **1991**, *22*, 529-536.
- (71) Walling, C.; Weil, T. The Ferric Ion Catalyzed Decomposition of Hydrogen Peroxide in Perchloric Acid Solution. *Int. J. Chem. Kinet.*, **1974**, *VI*, 507-516.
- (72) Walling, C.; Partch, R. E.; Weil, T. Kinetics of the Decomposition of Hydrogen Peroxide Catalyzed by Ferric Ethylenetetraacetate Complex. *Proc. Nat. Acad. Sci. USA*, **1975**, *72*, 140-142.
- (73) Walling, C.; Cleary, M. Oxygen Evolution as a Critical Test of Mechanism in the Ferric-Ion Catalyzed Decomposition of Hydrogen Peroxide. *Int. J. Chem. Kinet.*, **1977**, *IX*, 595-601.
- (74) Eary, L. E. Catalytic Decomposition of Hydrogen Peroxide by Ferric Ion in Dilute Sulfuric Acid Solutions. *Metallurg. Trans.*, **1985**, *16B*, 181-186.
- (75) Kremer, M. L. "Complex" versus "Free Radical" Mechanism for the Catalytic Decomposition of H<sub>2</sub>O<sub>2</sub> by Ferric Ions. *Int. J. Chem. Kinet.*, **1985**, *17*, 1299-1314.
- (76) Afanas'ev, I. B. *Superoxide Ion: Chemistry and Biological Implications*; CRC Press, Inc.: Boca Raton, 1989; pp 199.
- (77) Karakhanov, E. A.; Narin, S. Y.; Dedov, A. G. On the mechanism of catalytic hydroxylation of aromatic hydrocarbons by hydrogen peroxide. *Appl. Organomet. Chem.*, **1991**, *5*, 445-461.
- (78) Lin, S.-S.; Gurol, M. D. Catalytic Decomposition of Hydrogen Peroxide on Iron Oxide: Kinetics, Mechanism, and Implications. *Environ. Sci. Technol.*, **1998**, *32*, 1417-1423.
- (79) Jones, C. W. *Applications of Hydrogen Peroxide and Derivatives*; Royal Society of Chemistry: Cambridge, UK, 1999; pp 257.
- (80) Lee, Y.; Lee, C.; Yoon, J. High temperature dependence of 2,4-dichlorophenoxyacetic acid degradation by Fe<sup>3+</sup>/H<sub>2</sub>O<sub>2</sub> system. *Chemosphere*, **2003**, *51*, 963-971.
- (81) Malik, P. K. Oxidation of Safranin T in Aqueous Solution Using Fenton's Reagent: Involvement of an Fe(III) Chelate in the Catalytic Hydrogen Peroxide Oxidation of Safranin T. *J. Phys. Chem. A*, **2004**, *108*, 2675-2681.
- (82) Zhang, H.; Choi, H. J.; Huang, C.-P. Optimization of Fenton process for the treatment of landfill leachate. *J. Haz. Mater.*, **2005**, *B125*, 166-174.
- (83) Kusic, H.; Koprivanac, N.; Bozic, A. L.; Selanec, I. Photo-assisted Fenton type processes for the degradation of phenol: A kinetic study. *J. Haz. Mater.*, **2006**, *B136*, 632-644.
- (84) Smith, B. A.; Teel, A. L.; Watts, R. J. Mechanism for the destruction of carbon tetrachloride and chloroform DNAPLs by modified Fenton's reagent. *J. Contam. Hydr.*, **2006**, *85*, 229-246.
- (85) Chu, W.; Chan, K. H.; Kwan, C. Y.; Choi, K. Y. Degradation of atrazine by modified stepwise-Fenton processes. *Chemosphere*, **2007**, *67*, 755-761.
- (86) Barreiro, J. C.; Capelato, M. D.; Martin-Neto, L.; Hansen, H. C. B. Oxidative decomposition of atrazine by a Fenton-like reaction in a H<sub>2</sub>O<sub>2</sub>/ferrihydrite system. *Water Res.*, **2007**, *41*, 55-62.
- (87) Li, Y.-C.; Bachas, L. G.; Bhattacharyya, D. Selected Chloro-Organic Detoxifications by Polychelate (Poly(acrylic acid)) and Citrate-Based Fenton Reaction at Neutral pH Environment. *Ind. Eng. Chem. Res.*, **2007**, *46*, 7984-7992.

- (88) Apak, R. Life detection experiments of the Viking Mission on Mars can best be interpreted with a Fenton oxidation reaction composed of H<sub>2</sub>O<sub>2</sub> and Fe<sup>2+</sup> and iron-catalyzed decomposition of H<sub>2</sub>O<sub>2</sub>. *Int. J. Astrobiol.*, **2008**, *7*, 187-192.
- (89) Fan, H.-J.; Huang, S.-T.; Chung, W.-H.; Jan, J.-L.; Lin, W.-Y.; Chen, C.-C. Degradation pathways of crystal violet by Fenton and Fenton-like systems: Condition optimization and intermediate separation and identification. *J. Haz. Mater.*, **2009**, *171*, 1032-1044.
- (90) Lipczynska-Kochany, E.; Kochany, J. Effect of humic substances on the Fenton treatment of wastewater at acidic and neutral pH. *Chemosphere*, **2008**, *73*, 745-750.
- (91) Lewis, S.; Lynch, A.; Bachas, L.; Hampson, S.; Ormsbee, L.; Bhattacharyya, D. Chelate-Modified Fenton Reaction for the Degradation of Trichloroethylene in Aqueous and Two-Phase Systems. *Environ. Eng. Sci.*, **2009**, *26*, 849-859.
- (92) Masomboon, N.; Ratanatamskul, C.; Lu, M.-C. Chemical Oxidation of 2,6-Dimethylaniline in the Fenton Process. *Environ. Sci. Technol.*, **2009**, *43*, 8629-8634.
- (93) Samet, Y.; Ayadi, M.; Abdelhedi, R. Degradation of 4-Chloroguaiacol by Dark Fenton and Solar Photo-Fenton Advanced Oxidation Processes. *Water Environ. Res.*, **2009**, *81*, 2389-2397.
- (94) Garrido-Ramirez, E. G.; Theng, B. K. G.; Mora, M. L. Clays and oxide minerals as catalysts and nanocatalysts in Fenton-like reactions - A review. *Appl. Clay Sci.*, **2010**, *47*, 182-192.
- (95) Ratanatamskul, C.; Narkwittaya, S.; Masomboon, N.; Lu, M.-C. Oxidation of 2,6-dimethylaniline by the fluidized-bed Fenton process. *Reac. Kinet. Mech. Cat.*, **2010**, *101*, 301-311.
- (96) Wu, Y.; Zhou, S.; Qin, F.; Zheng, K.; Ye, X. Modeling the oxidation kinetics of Fenton's process on the degradation of humic acid. *J. Haz. Mater.*, **2010**, *179*, 533-539.
- (97) Zhu, S.-G.; Zhang, N.; Chen, X.; Cao, G.-P.; Yuan, W.-K. The mechanism and kinetics for the selective oxidation of glyoxal to produce glyoxalic acid by Fenton's reagent. *Reac. Kinet. Mech. Cat.*, **2010**, *99*, 325-333.
- (98) Samet, Y.; Wali, I.; Abdelhedi, R. Kinetic degradation of the pollutant guaiacol by dark Fenton and solar photo-Fenton processes. *Environ. Sci. Pollut. Res.*, **2011**, *18*, 1497-1507.
- (99) Simunovic, M.; Kusic, H.; Koprivanac, N.; Bozic, A. L. Treatment of simulated industrial wastewater by photo-Fenton process: Part II. The development of mechanistic model. *Chem. Eng. J.*, **2011**, *173*, 280-289.
- (100) Abdul, J. M.; Kumar, M.; Vigneswaran, S.; Kandasamy, J. Removal of metsulfuron methyl by Fenton Reagent. *J. Ind. Eng. Chem.*, **2012**, *18*, 137-144.
- (101) Venny; Gan, S.; Ng, H. K. Inorganic chelated modified-Fenton treatment of polycyclic aromatic hydrocarbon (PAH)-contaminated soils. *Chem. Eng. J.*, **2012**, *180*, 1-8.
- (102) Wang, C.; Liu, H.; Sun, Z. Heterogeneous Photo-Fenton Reaction Catalyzed by Nanosized Iron Oxides for Water Treatment. *Int. J. Photoenergy*, **2012**, 801694.
- (103) Wu, C.-H.; Hong, P. K. A.; Jian, M.-Y. Decolorization of Reactive Red 2 in Fenton and Fenton-like systems: effects of ultrasound and ultraviolet irradiation. *Reac. Kinet. Mech. Cat.*, **2012**, *106*, 11-24.
- (104) Doumic, L. I.; Haure, P. M.; Cassanello, M. C.; Ayude, M. A. Mineralization and efficiency in the homogeneous Fenton Orange G oxidation. *Appl. Catal. B: Environ.*, **2013**, *142-143*, 214-221.
- (105) Nidheesh, P. V.; Gandhimathi, R.; Ramesh, S. T. Degradation of dyes from aqueous solution by Fenton processes: a review. *Environ. Sci. Pollut. Res.*, **2013**, *20*, 2099-2132.

- (106) Babuponnusami, A.; Muthukumar, K. A review on Fenton and improvements to the Fenton process for wastewater treatment. *J. Environ. Chem. Eng.*, **2014**, *2*, 557-572.
- (107) Velo-Gala, I.; Lopez-Penalver, J. J.; Sanchez-Polo, M.; Rivera-Utrilla, J. Comparative study of oxidative degradation of sodium diatrizoate in aqueous solution by H<sub>2</sub>O<sub>2</sub>/Fe<sup>2+</sup>, H<sub>2</sub>O<sub>2</sub>/Fe<sup>3+</sup>, Fe(VI) and UV, H<sub>2</sub>O<sub>2</sub>/UV. *Chem. Eng. J.*, **2014**, *241*, 504-512.
- (108) Wang, Q.; Tian, S.; Ning, P. Degradation Mechanism of Methylene Blue in a Heterogeneous Fenton-like Reaction Catalyzed by Ferrocene. *Ind. Eng. Chem. Res.*, **2014**, *53*, 643-649.
- (109) Zhou, W.; Zhao, H.; Gao, J.; Meng, X.; Wu, S.; Qin, Y. Influence of a reagents addition strategy on the Fenton oxidation of rhodamine B: control of the competitive reaction of •OH. *RSC Adv.*, **2016**, *6*, 108791-108800.
- (110) Nakagawa, H.; Takagi, S.; Maekawa, J. Fered-Fenton process for the degradation of 1,4-dioxane with an activated carbon electrode: A kinetic model including active radicals. *Chem. Eng. J.*, **2016**, *296*, 298-405.
- (111) Litter, M. I.; Slodowicz, M. An overview on heterogeneous Fenton and photoFenton reactions using zerovalent iron materials. *J. Adv. Ox. Tech.*, **2017**, *20*, DOI: 10.1515/jaots-2016-0164.
- (112) Kremer, M. L. Strong Inhibition of the Fe<sup>3+</sup> + H<sub>2</sub>O<sub>2</sub> reaction by ethanol: evidence against the free radical theory. *Prog. React. Kinet. Mech.*, **2017**, *42*, 397-413.
- (113) Kremer, M. L. New kinetic analysis of the Fenton reaction: Critical examination of the free radical-chain reaction concept. *Prog. React. Kinet. Mech.*, **2019**, *44*, 289-299. doi.org/10.1177/1468678319860991.
- (114) Shinozawa, Y.; Heggo, D.; Ookawara, S.; Yoshikawa, S. Photo-Fenton Degradation of Carbofuran in Helical Tube Microreactor and Kinetic Modeling. *Ind. Eng. Chem. Res.*, **2020**, *59*, 3811-3819.
- (115) Cai, Q. Q.; Lee, B. C. Y.; Ong, S. L.; Hu, J. Y. Fluidized-bed Fenton technologies for recalcitrant industrial wastewater treatment- Recent advances, challenges and perspective. *Water Res.*, **2021**, *190*, 116692.
- (116) Russo, D. Kinetic Modeling of Advanced Oxidation Processes Using Microreactors: Challenges and Opportunities for Scale-Up. *Appl. Sci.*, **2021**, *11*, 1042.
- (117) Ribeiro, J. P.; Nunes, M. I. Recent trends and developments in Fenton processes for industrial wastewater treatment - A critical review. *Environ. Res.*, **2021**, *197*, 110957.
- (118) Wu, C.; Chen, W.; Gu, Z.; Li, Q. A review of the characteristics of Fenton and ozonation systems in landfill leachate treatment. *Sci. Total Environ.*, **2021**, *762*, 143131.
- (119) Raheb, I.; Manlla, M. S. Kinetic and thermodynamic studies of the degradation of methylene blue by photo-Fenton reaction. *Heliyon*, **2021**, *7*, e07427.
- (120) Roy, K.; Moholkar, V. S. p-nitrophenol degradation by hybrid advanced oxidation process of heterogeneous Fenton assisted hydrodynamic cavitation: Discernment of synergistic interactions and chemical mechanism. *Chemosphere*, **2021**, *283*, 13114.
- (121) Walling, S. A.; Um, W.; Corkhill, C. L.; Hyatt, N. C. Fenton and Fenton-like wet oxidation for degradation and destruction of organic radioactive wastes. *npj Mater. Degrad.*, **2021**, *5*, 50.
- (122) Kong, L.; Lemley, A. T. Modeling Evaluation of Carbaryl Degradation in a Continuously Stirred Tank Reactor by Anodic Fenton Treatment. *J. Agric. Food Chem.*, **2006**, *54*, 10061-10069.
- (123) Kong, L.; Lemley, A. T. Kinetic Modeling of 2,4-Dichlorophenoxyacetic Acid (2,4-D)

- Degradation in Soil Slurry by Anodic Fenton Treatment. *J. Agric. Food. Chem.*, **2006**, *54*, 3941-3950.
- (124) Brink, A.; Sheridan, C. M.; Harding, K. G. The Fenton oxidation of biologically treated paper and pulp mill effluents: A performance and kinetic study. *Proc. Safety Environ. Prot.*, **2017**, *107*, 206-215.
- (125) Ma, D.; Yi, H.; Lai, C.; Liu, X.; Huo, X.; An, Z.; Li, L.; Fu, Y.; Li, B.; Zhang, M.; Qin, L.; Liu, S.; Yang, L. Critical review of advanced oxidation processes in organic wastewater treatment. *Chemosphere*, **2021**, *275*, 130104.
- (126) Rodriguez, M. L.; Timokhin, V. I.; Contreras, S.; Chamarro, E.; Esplugas, S. Rate Equation for the degradation of nitrobenzene by 'Fenton-like' reagent. *Adv. Environ. Res.*, **2003**, *7*, 583-595.
- (127) Masomboon, N.; Ratanatamskul, C.; Lu, M.-C. Mineralization of 2,6-dimethylaniline by photoelectro-Fenton process. *Appl. Catal. A: General*, **2010**, *384*, 128-135.
- (128) Masomboon, N.; Ratanatamskul, C.; Lu, M.-C. Kinetics of 2,6-dimethylaniline oxidation by various Fenton processes. *J. Haz. Mater.*, **2011**, *192*, 347-353.
- (129) Wang, H.; Zhao, Y.; Su, Y.; Li, T.; Yao, M.; Qin, C. Fenton-like degradation of 2,4-dichlorophenol using calcium peroxide particles: performance and mechanisms. *RSC Adv.*, **2017**, *7*, 4563-4571.
- (130) Yu, S.; Gu, X.; Lu, S.; Xue, Y.; Zhang, X.; Xu, M.; Qiu, Z.; Sui, Q. Degradation of phenanthrene in aqueous solution by a persulfate/percarbonate system activated with CA chelated-Fe(II). *Chem. Eng. J.*, **2018**, *333*, 122-131.
- (131) Yang, Z.; Qian, J.; Yu, A.; Pan, B. Singlet oxygen mediated iron-based Fenton-like catalysis under nanoconfinement. *Proc. Nat. Acad. Sci. USA*, **2019**, *116*, 6659-6664.
- (132) Yang, Z.; Yan, Y.; Yu, A.; Pan, B.; Pignatello, J. J. Revisiting the phenanthroline and ferrozine colorimetric methods for quantification of Fe(II) in Fenton reactions. *Chem. Eng. J.*, **2020**, *391*, 123592.
- (133) Zhou, P.; Ren, W.; Nie, G.; Li, X.; Duan, X.; Y., Z.; Wang, S. Fast and Long-Lasting Iron(III) Reduction by Boron Toward Green and Accelerated Fenton Chemistry. *Angew. Chem. Int. ed.*, **2020**, *59*, 16517-16526.
- (134) Arts, A.; Schmuhl, R.; de Groot, M. T.; van der Schaaf, J. Fast initial oxidation of formic acid by the Fenton reaction under industrial conditions. *J. Water Proc. Eng.*, **2021**, *40*, 101780.
- (135) Yang, R.; Zeng, G.; Xu, Z.; Zhou, Z.; Huang, J.; Fu, R.; Lyu, S. Comparison of naphthalene removal performance using H<sub>2</sub>O<sub>2</sub>, sodium percarbonate and calcium peroxide oxidants activated by ferrous ions and degradation mechanism. *Chemosphere*, **2021**, *283*, 131209.
- (136) Gen, M.; Zhang, R.; Chan, C. K. Nitrite/Nitrous Acid Generation from the Reaction of Nitrate and Fe(II) Promoted by Photolysis of Iron-Organic Complexes. *Environ. Sci. Technol.*, **2021**, *55*, 15715-15723.
- (137) Wang, Y.; Wang, C.; Shi, S.; Fang, S. Improved removal performance and mechanism investigation of papermaking wastewater treatment using manganese enhanced Fenton reaction. *Water Sci. Technol.*, **2018**, *77*, 2509-2516.
- (138) Friedrich, L. C.; Mendes, M. A.; Silva, V. O.; Zanta, C. L. P. S.; Machulek, A.; Quina, F. H. Mechanistic Implications of Zinc(II) Ions on the Degradation of Phenol by the Fenton Reaction. *J. Braz. Chem. Soc.*, **2012**, *23*, 1372-1377.
- (139) Sheydaei, M.; Aber, S.; Khataee, A. Degradation of amoxicillin in aqueous solution using

- nanolipidocrocite chips/H<sub>2</sub>O<sub>2</sub>/UV: Optimization and kinetics studies. *J. Ind. Eng. Chem.*, **2014**, *20*, 1772-1778.
- (140) Gasmi, I.; Kerboua, K.; Haddour, N.; Hamdaoui, O.; Alghymah, A.; Buret, F. Kinetic pathways of iron electrode transformations in Galvano-Fenton process: A mechanistic investigation of in-situ catalyst formation and regeneration. *J. Taiwan Inst. Chem. Eng.*, **2020**, *116*, 81-91.
- (141) Gasmi, I.; Kerboua, K.; Haddour, N.; Hamdaoui, O.; Alghyamah, A.; Buret, F. The Galvano-Fenton process: Experimental insights and numerical mechanistic investigation applied to the degradation of acid orange 7. *Electrochim. Acta*, **2021**, *373*, 137897.
- (142) Gholami, M.; Shomali, A.; Souraki, B. A.; Pendashteh, A. Advanced numerical kinetic model for predicting COD removal and optimization of pulp and paper wastewater treatment by Fenton Process. *Int. J. Environ. Analyt. Chem.*, **2020**, 03067319. <https://doi.org/10.1080/03067319.2020.1759565>.
- (143) Jayson, G. G.; Keene, J. P.; Stirling, D. A.; Swallow, A. J. Pulse-Radiolysis Study of Some Unstable Complexes of Iron. *Trans. Faraday Soc.*, **1969**, *65*, 2453-2464.
- (144) Rush, J. D.; Bielski, B. H. J. Pulse Radiolytic Studies of the Reactions of HO<sub>2</sub>/O<sub>2</sub><sup>-</sup> with Fe(II)/Fe(III) Ions. The Reactivity of HO<sub>2</sub>/O<sub>2</sub><sup>-</sup> with Ferric Ions and Its Implication on the Occurrence of the Haber-Weiss Reaction. *J. Phys. Chem.*, **1985**, *89*, 5062-5066. [doi.org/10.1021/j100269a035](https://doi.org/10.1021/j100269a035).
- (145) Burbano, A. A.; Dionysiou, D. D.; Suidan, M. T.; Richardson, T. L. Oxidation kinetics and effect of pH on the degradation of MTBE with Fenton reagent. *Water Res.*, **2005**, *39*, 107-118.
- (146) Burbano, A. A.; Dionysiou, D. D.; Suidan, M. T. Effect of oxidant-to-substrate ratios on the degradation of MTBE with Fenton reagent. *Water Res.*, **2008**, *42*, 3225-3239.
- (147) Kusic, H.; Koprivanac, N.; Horvat, S.; Bakija, S.; Bozic, A. L. Modeling dye degradation kinetic using dark- and photo-Fenton type processes. *Chem. Eng. J.*, **2009**, *155*, 144-154.
- (148) Kusic, H.; Peternel, I.; Ukić, S.; Koprivanac, N.; Bolanca, T.; Papic, S.; Bozic, A. L. Modeling of iron activated persulfate oxidation treating reactive azo dye in water matrix. *Chem. Eng. J.*, **2011**, *172*, 109-121.
- (149) Venny; Gan, S.; Ng, H. K. Current status and prospects of Fenton oxidation for the decontamination of persistent organic pollutants (POPs) in soils. *Chem. Eng. J.*, **2012**, *213*, 295-317.
- (150) Ghafoori, S.; Mehrvar, M.; Chan, P. K. Photoassisted Fenton-like degradation of aqueous poly(acrylic acid): From mechanistic kinetic model to CFD modeling. *Chem. Eng. Res. Desg.*, **2013**, *91*, 2617-2629.
- (151) Lakey, P. S. J.; Berkemeier, T.; Tong, H.; Arangio, A. M.; Lucas, K.; Pöschl, U.; Shiraiwa, M. Chemical exposure-response relationship between air pollutants and reactive oxygen species in the human respiratory tract. *Sci. Rpts.*, **2016**, *6*, 32916.
- (152) Farshchi, M. E.; Aghdasinia, H.; Khataee, A. Modeling of heterogeneous Fenton process for dye degradation in a fluidized-bed reactor: Kinetics and mass transfer. *J. Cleaner Prod.*, **2018**, *182*, 644-653.
- (153) Kochany, J.; Lipczynska-Kochany, E. Fenton Reaction in the Presence of Humates. Treatment of Highly Contaminated Wastewater at Neutral pH. *Environ. Technol.*, **2007**, *28*, 1007-1013.
- (154) Pignatello, J. J.; Oliveros, E.; MacKay, A. Advanced Oxidation Processes for Organic Contaminant Destruction Based on the Fenton Reaction and Related Chemistry. *Crit. Rev.*

- Environ. Sci. Technol.*, **2006**, *36*, 1-84.
- (155) Tong, H.; Lakey, P. S. J.; Arangio, A. M.; Socorro, J.; Kampf, C. J.; Berkemeier, T.; Brune, W. H.; Pöschl, U.; Shiraiwa, M. Reactive oxygen species formed in aqueous mixtures of secondary organic aerosols and mineral dust influencing cloud chemistry and public health in the Anthropocene. *Faraday Disc.*, **2017**, *200*, 251-270.
- (156) Zimbron, J. A.; Reardon, K. F. Fenton's oxidaton of pentachlorophenol. *Water Res.*, **2009**, *43*, 1831-1840.
- (157) Fang, T.; Lakey, P. S. J.; Rivera-Rios, J. C.; Keutsch, F. N.; Shiraiwa, M. Aqueous-Phase Decomposition of Isoprene Hydroxy Hydroperoxide and Hydroxyl Radical Formation by Fenton-like reactions with Iron Ions. *J. Phys. Chem. A*, **2020**, *124*, 5230-5236.
- (158) Ouyang, Z.; Yang, C.; He, J.; Yao, Q.; Zhang, B.; Wang, H.; Jiang, Y.; Zhou, J.; Deng, Y.; Liu, Y.; Yang, J.; Lu, G.; Dang, Z. Homogeneous photocatalytic degradation of sulfamethazine induced by Fe(III)-carboxylate complexes: Kinetics, mechanism and products. *Chem. Eng. J.*, **2020**, *402*, 126122.
- (159) Möller, D.; Mauersberger, G. Cloud Chemistry Effects on Tropospheric Photooxidants in Polluted Atmosphere - Model Results. *J. Atmos. Chem.*, **1992**, *14*, 153-165.
- (160) Vorontsov, A. V. Advancing Fenton and photo-Fenton water treatment through the catalyst design. *J. Haz. Mater.*, **2019**, *372*, 103-112.
- (161) Graedel, T. E.; Mandich, M. L.; Weschler, C. J. Kinetic Model Studies of Atmospheric Droplet Chemistry 2. Homogeneous Transition Metal Chemistry in Raindrops. *J. Geophys. Res. D*, **1986**, *91*, 5205-5221.
- (162) Sychev, A. Y.; Isak, V. G. Iron compounds and the mechanisms of the homogeneous catalysis of the activation of O<sub>2</sub> and H<sub>2</sub>O<sub>2</sub> and of the oxidation of organic substrates. *Russ. Chem. Rev.*, **1995**, *64*, 1105-1129.
- (163) Kozlov, Y. N.; Nadezhdin, A. D.; Pourmal, A. P. Initiation Process in the System Fe<sup>3+</sup> + H<sub>2</sub>O<sub>2</sub>. *Int. J. Chem. Kinet.*, **1974**, *VI*, 383-394. doi.org/10.1002/kin.550060308.
- (164) Herrera, F.; Kiwi, J.; Lopez, A.; Nadtochenko, V. Photochemical Decoloration of Remazol Brilliant Blue and Uniblue A in the Presence of Fe<sup>3+</sup> and H<sub>2</sub>O<sub>2</sub>. *Environ. Sci. Technol.*, **1999**, *33*, 3145-3151.
- (165) Kiwi, J.; Lopez, A.; Nadtochenko, V. Mechanism and Kinetics of the OH-Radical Invervention during Fenton Oxidation in the Presence of a Significant Amount of Radical Scavenger (Cl<sup>-</sup>). *Environ. Sci. Technol.*, **2000**, *34*, 2162-2168.
- (166) Cahill, A. E.; Taube, H. The Use of Heavy Oxygen in the Study of Reactions of Hydrogen Peroxide. *J. Am. Chem. Soc.*, **1952**, *74*, 2312-2318.
- (167) Walling, C. Fenton's Reagent Revisited. *Acc. Chem. Res.*, **1975**, *8*, 125-131.
- (168) Pignatello, J. J. Dark and Photoassisted Fe<sup>3+</sup>-Catalyzed Degradation of Chlorophenoxy Herbicides by Hydrogen Peroxide. *Environ. Sci. Technol.*, **1992**, *26*, 944-951.
- (169) Safarzadeh-Amiri, A.; Bolton, J. R.; Cater, S. R. The Use of Iron in Advanced Oxidation Processes. *J. Adv. Oxid. Technol.*, **1996**, *1*, 18-26.
- (170) Lu, M.-C.; Chen, J.-N.; Chang, C.-P. Effect of Inorganic Ions on the Oxidation of Dichlorvos Insecticide with Fenton's Reagent. *Chemosphere*, **1997**, *35*, 2285-2293.
- (171) Lu, M.-C.; Chen, J.-N.; Chang, C.-P. Oxidation of dichlorvos with hydrogen peroxide using ferrous ion as catalyst. *J. Haz. Mater.*, **1999**, *B65*, 277-288.
- (172) Chamarro, E.; Marco, A.; Esplugas, S. Use of Fenton reagent to Improve Organic Chemical Biodegradability. *Water Res.*, **2001**, *35*, 1047-1051.
- (173) Yoon, J.; Lee, Y.; Kim, S. Investigation of the reaction pathway of OH radicals produced

- by Fenton oxidation in the conditions of wastewater treatment. *Water Sci. Technol.*, **2001**, *44*, 15-21.
- (174) Neyens, E.; Baeyens, J. A review of classic Fenton's peroxidation as an advanced oxidation technique. *J. Haz. Mater.*, **2003**, *B98*, 33-50.
- (175) Xu, X.-R.; Zhao, Z.-Y.; Li, X.-Y.; Gu, J.-D. Chemical oxidative degradation of methyl tert-butyl ether in aqueous solution by Fenton's reagent. *Chemosphere*, **2004**, *55*, 73-79.
- (176) Perez-Benito, J. F. Iron(III)-Hydrogen Peroxide Reaction: Kinetic Evidence of a Hydroxyl-Mediated Chain Mechanism. *J. Phys. Chem. A*, **2004**, *108*, 4853-5858.
- (177) Ntampeglitis, K.; Riga, A.; Karayannis, V.; Bontozoglou, V.; Papapolymerou, G. Decolorization kinetics of Procion H-exl dyes from textile dyeing using Fenton-like reactions. *J. Haz. Mater.*, **2006**, *136*, 75-84.
- (178) Siedlecka, E. M.; Stepnowski, P. Decomposition rates of methyl tert-butyl ether and its by-products by the Fenton system in saline wastewaters. *Sep. Purif. Tech.*, **2006**, *52*, 317-324.
- (179) Siedlecka, E. M.; Wieckowska, A.; Stepnowski, P. Influence of Inorganic Ions on MTBE Degradation by Fenton's Reagent. *J. Haz. Mater.*, **2007**, *147*, 497-502.
- (180) Behnajady, M. A.; Modirshahla, N.; Ghanbary, F. A kinetic model for the decolorization of C.I. Acid Yellow 23 by Fenton Process. *J. Haz. Mater.*, **2007**, *1148*, 98-102.
- (181) Nogueira, R. F. P.; Trovo, A. G.; de Silva, R. A.; Villa, R. D. Fundamentos e Aplicacoes Ambientais dos Processos Fenton e Foto-Fenton. *Quim. Nova*, **2007**, *30*, 400-408.
- (182) Jung, Y. S.; Lim, W. T.; Park, J.-Y.; Kim, Y.-H. Effect of pH on Fenton and Fenton-like oxidation. *Environ. Technol.*, **2009**, *30*, 183-190.
- (183) Masomboon, N.; Ratanatamskul, C.; Lu, M.-C. Chemical oxidation of 2,6-dimethylaniline by electrochemically generated Fenton's reagent. *J. Haz. Mater.*, **2010**, *176*, 92-98.
- (184) Navalon, S.; Alvaro, M.; Garcia, H. Heterogeneous Fenton catalysts based on clays, silicas and zeolites. *Appl. Catal. B: Environ.*, **2010**, *99*, 1-26.
- (185) Rojas, M. R.; Perez, F.; Whitley, D.; Arnold, R. G.; Saez, A. E. Modeling of Advanced Oxidation of Trace Organic Contaminants by Hydrogen Peroxide Photolysis and Fenton's Reaction. *Ind. Eng. Chem. Res.*, **2010**, *49*, 11331-11343.
- (186) Hussain, S.; Aneggi, E.; Goi, D. Catalytic activity of metals in heterogeneous Fenton-like oxidation of wastewater contaminants: a review. *Environ. Chem. Lett.*, **2021**, *19*, 2405-2424. <https://doi.org/10.1007/s10311-021-01185-z>.
- (187) De Laat, J.; Le, T. G. Kinetics and Modeling of the Fe(III)/H<sub>2</sub>O<sub>2</sub> System in the Presence of Sulfate in Acidic Aqueous Solutions. *Environ. Sci. Technol.*, **2005**, *39*, 1811-1818.
- (188) Shen, J.; Griffiths, P. T.; Campbell, S. J.; Utinger, B.; Kalberer, M.; Paulson, S. E. Ascorbate oxidation by iron, copper and reactive oxygen species: review, model development, and derivation of key rate constants. *Sci. Reports*, **2021**, *11*, 7417.
- (189) Lunar, L.; Sicilia, D.; Rubio, S.; Perez-Bendito, D.; Nickel, U. Degradation of Photographic Developers by Fenton's Reagent: Condition Optimization and Kinetics for Metal Oxidation. *Water Res.*, **2000**, *34*, 1791-1802.
- (190) Lu, M.-C.; Chang, Y.-F.; Chen, I.-M.; Huang, Y.-Y. Effect of chloride ions on the oxidation of aniline by Fenton's reagent. *J. Environ. Manag.*, **2005**, *75*, 177-182.
- (191) Anotai, J.; Lu, M. C.; Chewprecha, P. Kinetics of aniline degradation by Fenton and electro-Fenton processes. *Water Res.*, **2006**, *40*, 1841-1847.
- (192) Siedlecka, E. M.; Stepnowski, P. Effect of Chlorides and Sulfates on the Performance of a Fe<sup>3+</sup>/H<sub>2</sub>O<sub>2</sub> Fenton-Like System in the Degradation of Methyl Tert-Butyl Ether and its Byproducts. *Water Environ. Res.*, **2007**, *79*, 2318-2324.



- (193) Eren, Z.; Acar, F. N.; Ince, N. H. Fenton and Fenton-like oxidation of CI Basic Yellow 51: a comparative study. *Color. Technol.*, **2010**, *126*, 337-341.
- (194) Ghosh, P.; Samanta, A. N.; Ray, S. COD Reduction of Petrochemical Industry Wastewater Using Fenton's Oxidation. *Can J. Chem. Eng.*, **2010**, *88*, 1021-1026.
- (195) Su, C.-C.; Bellotindos, L. M.; Chang, A.-T.; Lu, M.-C. Degradation of acetaminophen in an aerated Fenton reactor. *J. Taiwan Inst. Chem. Eng.*, **2013**, *44*, 310-316.
- (196) Jung, H.-J.; Hong, J.-S.; Suh, J.-K. A comparison of fenton oxidation and photocatalyst reaction efficiency for humic acid degradation. *J. Ind. Eng. chem.*, **2013**, *19*, 1325-1330.
- (197) Andreozzi, R.; D'Apuzzo, A.; Marotta, R. A kinetic model for the degradation of benzothiazole by Fe<sup>3+</sup>-photo-assisted Fenton process in a completely mixed batch reactor. *J. Haz. Mater.*, **2000**, *B80*, 241-257.
- (198) Wiegand, H. L.; Orths, C. T.; Kerpen, K.; Lutze, H. V.; Schmidt, T. C. Investigation of the Iron-Peroxo Complex in the Fenton Reaction: Kinetic Indication, Decay Kinetics, and Hydroxyl Radical Yields. *Environ. Sci. Technol.*, **2017**, *51*, 14321-14329.
- (199) Kerboua, K.; Hamdaoui, O.; Haddour, N.; Alghyamah, A. Simultaneous Galvanic Generation of Fe<sup>2+</sup> Catalyst and Spontaneous Energy Release in the Galvano-Fenton Technique: A Numerical Investigation of Phenol's Oxidation and Energy Production and Saving. *Catalysts*, **2021**, *11*, 943.
- (200) Qin, H.; Fan, J.; Mao, S. Exploring the mechanism of the Fe(III)-activated Fenton-like reaction based on a quantitative study. *New J. Chem.*, **2020**, *44*, 8952-8959.
- (201) Ghiselli, G.; Jardim, W. F.; Litter, M. I.; Mansilla, H. D. Destruction of EDTA using Fenton and photo-Fenton-like reactions under UV-A irradiation. *J. Photochem. Photobiol. A*, **2004**, *167*, 59-67.
- (202) Kang, N.; Hua, I. Enhanced chemical oxidation of aromatic hydrocarbons in soil systems. *Chemosphere*, **2005**, *61*, 909-922.
- (203) Chen, Y.; Miller, C. J.; Waite, T. D. Heterogeneous Fenton Chemistry Revisited: Mechanistic Insights from Ferrihydrite-Mediated Oxidation of Formate and Oxalate. *Environ. Sci. Technol.*, **2021**, *55*, 14414-14425. doi.org/10.1021/acs.est.1c00284.
- (204) De Laat, J.; Le, T. G. Effects of chloride ions on the iron(III)-catalyzed decomposition of hydrogen peroxide and on the efficiency of the Fenton-like oxidation process. *Appl. Catal. B: Environmental*, **2006**, *66*, 137-146.
- (205) Benitez, F. J.; Real, F. J.; Acero, J. L.; Garcia, C.; Llanos, E. M. Kinetics of phenylurea herbicides oxidation by Fenton and photo-Fenton processes. *J. Chem. Technol. Biotech.*, **2007**, *82*, 65-73.
- (206) De Laat, J.; Gallard, H. Catalytic Decomposition of Hydrogen Peroxide by Fe(III) in Homogeneous Aqueous Solution: Mechanism and Kinetic Modeling. *Environ. Sci. Technol.*, **1999**, *33*, 2726-2732. doi.org/10.1021/es981171v.
- (207) Gallard, H.; De Laat, J. Kinetic Modelling of Fe(III)/H<sub>2</sub>O<sub>2</sub> Oxidation Reactions in Dilute Aqueous Solution Using Atrazine as a Model Organic Compound. *Water Res.*, **2000**, *34*, 3107-3116.
- (208) Giannakis, S.; Lopez, M. I. P.; Spuhler, D.; Perez, J. A. S.; Ibanez, P. F.; Pulgarin, C. Solar disinfection is an augmentable, in situ-generated photo-Fenton reaction-Part 1: A review of the mechanisms and the fundamental aspects of the process. *Appl. Catal. B: Environ.*, **2016**, *199*, 199-223.
- (209) Giannakis, S.; Liu, S.; Carratala, A.; Rtimi, S.; Bensimon, M.; Pulgarin, C. Effect of Fe(II)/Fe(III) species, pH, irradiance and bacterial presence on viral inactivation in

- wastewater by the photo-Fenton process: Kinetic modeling and mechanistic interpretation. *Appl. Catal. B: Environ.*, **2017**, *204*, 156-166.
- (210) Martin, L. R.; Easton, M. P.; Foster, J. W.; Hill, M. W. Oxidation of Hydroxymethanesulfonic Acid by Fenton's reagent. *Atmos. Environ.*, **1989**, *23*, 563-568.
- (211) Amme, M.; Bors, W.; Michel, C.; Stettmaier, K.; Rasmussen, G.; Betti, M. Effects of Fe(II) and Hydrogen Peroxide Interaction upon Dissolving UO<sub>2</sub> under Geologic Repository Conditions. *Environ. Sci. Technol.*, **2005**, *39*, 221-229.
- (212) Ananzeh, N. A.; Bergendahl, J. A.; Thompson, R. W. Kinetic Model for the Degradation of MTBE by Fenton's Oxidation. *Environ. Chem.*, **2006**, *3*, 40-47.
- (213) Banerjee, P.; DasGupta, S.; De, S. Kinetic Study of Advanced Oxidation of Eosin Dye by Fenton's Reagent. *Int. J. Chem. Reactor Eng.*, **2008**, *6*, A69.
- (214) Lee, C.; Yoon, J. Temperature dependence of hydroxyl radical formation in the  $h\nu/\text{Fe}^{3+}/\text{H}_2\text{O}_2$  and  $\text{Fe}^{3+}/\text{H}_2\text{O}_2$  systems. *Chemosphere*, **2004**, *56*, 923-934.
- (215) Farinelli, G.; Di Lucia, A.; Kaila, V. R. I.; MacLachan, M. J.; Tiraferri, A. Fe-Chitosan complexes for oxidative degradation of emerging contaminants in water: Structure, activity, and reaction mechanism. *J. Haz. Mater.*, **2021**, *408*, 124662.
- (216) Attiogbe, F. K.; Francis, R. C. Hydrogen peroxide decomposition in bicarbonate solution catalyzed by ferric citrate. *Can. J. Chem.*, **2011**, *98*, 1289-1296.
- (217) Park, J. S. B.; Wood, P. M.; Davies, M. J.; Gilbert, B. C.; Whitwood, A. C. A Kinetic and ESR Investigation of Iron(II) Oxalate Oxidation by Hydrogen Peroxide and Dioxygen as a Source of Hydroxyl Radicals. *Free Rad. Res.*, **1997**, *27*, 447-458.
- (218) Gabricevic, M.; Lente, G.; Fábian, I. Hydrogen Isotope Exchange of Chlorinated Ethylenes in Aqueous Solution: Possibly a Termolecular Liquid Phase Reaction. *J. Phys. Chem. A*, **2015**, *119*, 12627-12634.
- (219) De Laat, J.; Dao, Y. H.; El Najjar, N. H.; Daou, C. Effect of some parameters on the rate of the catalyzed decomposition of hydrogen peroxide by iron(III)-nitriloacetate in water. *Water Res.*, **2011**, *45*, 5654-5664.
- (220) Zhang, P.; Yuan, S. Production of hydroxyl radicals from abiotic oxidation of pyrite by oxygen under circumneutral conditions in the presence of low-molecular-weight organic acids. *Geochim. Cosmochim. Acta*, **2017**, *218*, 153-166.